Electronic Supplementary Material (ESI) for Dalton Transactions.

Supporting Information for

Phosphate Selective Binding and Sensing by Halogen Bonding Tripodal Cu(II) Metallo-receptors in Aqueous Media.

Hena Bagha, Robert Hein, Jason Y. C. Lim, William K. Myers, Mark R. Sambrook and Paul D. Beer*

Email: paul.beer@chem.ox.ac.uk

Contents

S1. General Considerations

S1.1 Solvents and Reagents

All solvents and reagents were purchased from commercial suppliers and used without further purification. Dry solvents were obtained by passing through a MBraun MPSP-800 column, degassed with nitrogen and used immediately. Water was de-ionized and micro filtered using a Milli-Q® Millipore machine. All tetrabutylammonium (TBA) salts as well as $[Cu(MeCN)_4][PF_6]$, and $Cu(OTf)_2$ were stored in a vacuum desiccator at room temperature with P_2O_5 desiccant prior to use. Triethylamine was distilled from and stored over KOH pellets. Thin layer chromatography (TLC) analysis was performed using Merck® aluminium-backed DC 60 F254 0.2 mm silica precoated plates, with spots visualised under UV light (254 nm) and/ or staining with basified aqueous $KMnO_4$ solution followed by gentle heating. Column chromatography was undertaken on Merck® silica gel 60 under a positive pressure of nitrogen. Preparative TLC was performed using Analtech glass-backed pre-coated plates (20 × 20 cm, 0.1 cm silica thickness). Where mixtures of solvents were used, ratios are reported by volume. Any literature procedures used to prepare known compounds are referenced in the text. Tris(benzyltriazolemethyl)amine (TBTA) was synthesised as described[1] and stored under ambient conditions.

S1.2 Instrumentation

^1H and ^{13}C NMR spectra were recorded using Bruker Avance III 400 HD nanobay NMR spectrometers (Hg400 or Venus400) each equipped with a 9.4 T magnet, or a Bruker Avance III 500 machine (AVD500) equipped with a 11.75 T magnet (and cryoprobe) at T = 298 K. Chemical shifts are quoted in parts per million (ppm) relative to the residual solvent peak. Low and high resolution ESI mass spectra were recorded on a Waters LCT premier spectrometer and a Bruker µTOF spectrometer respectively. All pH measurements of solutions of complexes in aqueous and aqueous-organic media were performed using a Hanna® pH meter. Isothermal titration calorimetry experiments were performed on a Microcal PEAQ-ITC automated system. EPR spectra were recorded using a Bruker EMXmicro continuous wave (CW) spectrometer (X-band) at T = 85 K. UV-vis spectra were recorded on a T60U (PG Instruments Ltd) spectrophotometer at T = 293 K, using a Hellma quartz cuvette with path length of 1 cm.

S2. Experimental Procedures

Tris(TEG)-appended HB Cu(II) tripod, **1H**·2OTf

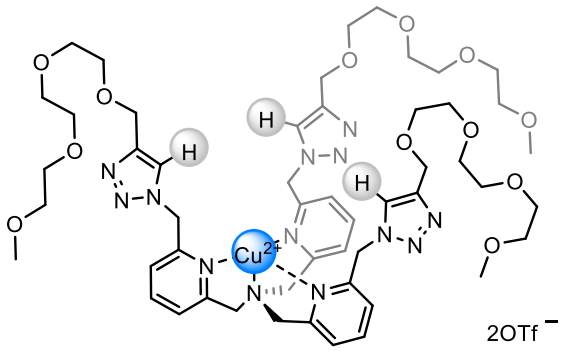

To tripodal ligand **6H** (205 mg, 0.2 mmol) in a 1:1 mixture of CH_2Cl_2/MeOH (6 mL) was added copper(II) trifluoromethansulfonate (72.3 mg, 0.2 mmol) and the solution stirred at room temperature under a N_2 atmosphere for 3 hours. Removal of the solvent *in vacuo* afforded metallo-tripodal receptor **1H**·2OTf as a deep blue oil, which solidified to a dark blue crystalline residue upon drying under high vacuum (274 mg, quantitative). **UV-vis** (CH_3CN/ H_2O 6:4 *v/v*, 10 mM HEPES, λ_{max}/ nm, (ε/ M^{-1} cm^{-1})): 639 (125), 760 (98); **EPR** (CH_3CN/ H_2O 6:4 *v/v*, 10 mM HEPES, 85 K): $g\parallel$ = 2.225, $g\perp$ = 2.065, $A\parallel$ = 182.0 x 10^{-4} cm^{-1}; **HR-MS** (ESI +ve) *m/z:* 562.24714 ($[M - 2OTf]^{2+}$, $C_{51}H_{75}N_{13}O_{12}{}^{63}Cu$ calc. 562.24716).

Tris(TEG)-appended XB Cu(II) tripod, **1I**·2OTf

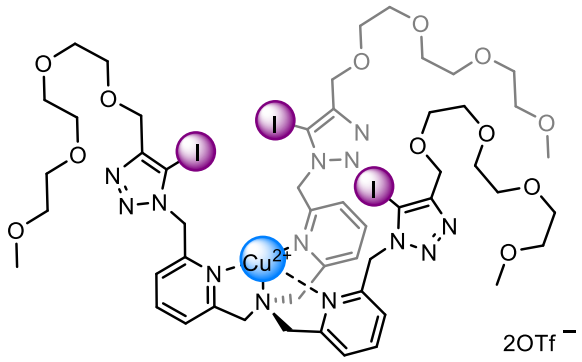

To tripodal ligand **6I** (199 mg, 0.139 mmol) in a 1:1 mixture of CH_2Cl_2/MeOH (6 mL) was added copper(II) trifluoromethansulfonate (50.3 mg, 0.139 mmol) and the solution stirred at room temperature under a N_2 atmosphere for 3 hours. Removal of the solvent *in vacuo* afforded metallo-tripodal receptor **1I**·2OTf as a deep blue oil, which solidified to a dark blue crystalline residue upon drying under high vacuum (248 mg, quantitative). **UV-vis** (CH_3CN/ H_2O 6:4 *v/v*, 10 mM HEPES, λ_{max}/ nm, (ε/ M^{-1} cm^{-1})): 647 (117), 775 (91); **EPR** (CH_3CN/ H_2O 6:4 *v/v*, 10

mM HEPES, 85 K): $g\|$ = 2.225, $g\perp$ = 2.065, $A\|$ = 183.0 x 10^{-4} cm^{-1}; **HR-MS** (ESI +ve) *m/z:* 751.09167 ($[M - 2OTf]^{2+}$, $C_{51}H_{72}N_{13}O_{12}I_3{}^{63}Cu$ calc. 751.09212).

(6-(azidomethyl)pyridine-2-yl)methanol, **2**[2]

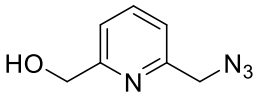

This literature compound was prepared using modified synthetic procedures: to a solution of **1** (1.58 g, 7.82 mmol) in dry, degassed DMF (40 mL) was added NaN_3 (1.02 g, 15.6 mmol) and the reaction stirred under a N_2 atmosphere at 80 °C overnight. Thereafter, azeotropic removal of the solvent *in vacuo* with toluene produced a dark yellow residue which was redissolved in ethyl acetate (20 mL). The resultant precipitate was removed *via* filtration through a pad of celite and the celite thoroughly washed with ethyl acetate. Removal of the solvent *in vacuo* afforded the target compound **2** in excellent purity as a deep yellow oil which was dried *in vacuo* at less than 7 mbar for 2 days (1.13 g, 88 % yield). **^{1}H NMR** (400 MHz, $CDCl_3$) *δ* (ppm): 7.73 (1H, t, ^3J = 8.0 Hz, pyridine Ar*H*), 7.26 (1H, d, ^3J = 8.0 Hz, pyridine Ar*H*), 7.22 (1H, d, ^3J = 8.0 Hz, pyridine Ar*H*), 4.78 (2H, s, pyridine CH_2), 4.49 (2H, s, pyridine CH_2), 3.70 (1H, br. s, CH_2-O*H*); **^{13}C NMR** (125 MHz, $CDCl_3$) δ (ppm): 159.4, 154.5, 137.5, 120.3, 119.6, 63.8, 54.9; **LR-MS** (ESI +ve) *m/z*: 165.1 ($[M+H]^+$, $C_7H_9N_4O$ calc. 165.1)

2,5,8,11-tetraoxatetradec-13-yne, **3**[3]

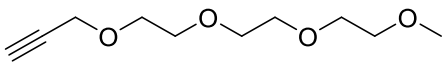

To a stirring solution of triethylene glycol monomethyl ether (2.0 g, 12.2 mmol) in dry degassed THF (3 mL) at 0 °C, was added a suspension of potassium *tert*-butoxide (1.56 g, 13.9 mmol) in 25 mL THF. Separately 1.82 mL of propargyl bromide (24.2 mmol) was dissolved in THF (50 mL) and then added dropwise to the solution. The reaction mixture was stirred at room temperature under a N_2 atmosphere for 24 h. Thereafter, ethyl acetate (200 mL) was added and the organics washed with brine (3 x 75 mL). The separated organic layer was dried over $MgSO_4$ and filtered. Removal of the solvent *in vacuo* afforded **12** in good purity as a pale yellow oil (1.69 g, 69 %). **^{1}H NMR** (500 MHz, $CDCl_3$) δ (ppm): 4.21 (2H, d, ^4J = 2.4 Hz, CH_2C≡C), 3.55 – 3.71 (12H, m, TEG alkyl-CH_2), 3.38 (3H, s, TEG alkyl-CH_3), 2.43 (1H, t, ^4J = 2.4 Hz, C≡C*H*); **^{13}C NMR** (125 MHz, $CDCl_3$) δ (ppm): 79.6, 74.4, 71.9, 70.6, 70.5, 70.4, 69.0,

59.0, 58.3, one peak missing, presumed overlapped; **HR-MS** (ESI +ve) *m/z*: 203.12779 ([M + H]$^+$, $C_{10}H_{19}O_4$ calc. 203.12779).

TEG-appended HB 'hydroxy-arm' precursor, **4H**

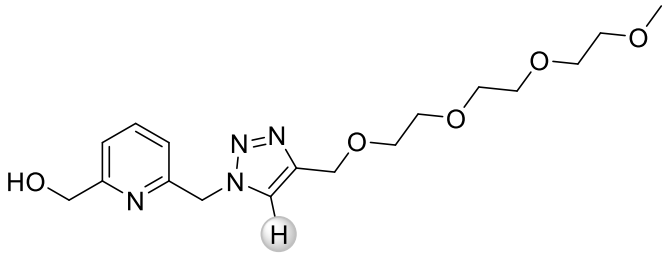

To a solution of (6-(azidomethyl)pyridine-2-yl)methanol **2** (350 mg, 2.13 mmol) and TEG alkyne **3** (431 mg, 2.13 mmol) in dry degassed THF (5 mL) was added $[Cu(MeCN)_4][PF_6]$ (397 mg, 1.07 mmol) and diisopropylethylamine (DIPEA) (0.18 mL, 1.07 mmol) and the mixture stirred at room temperature under a N_2 atmosphere for 2 days. The reaction mixture was diluted with CH_2Cl_2 (25 mL) and washed with $NH_4OH_{(aq)}$ (3 x 20 mL), brine (2 x 20 mL) and dried over $MgSO_4$. After removal of the solvent *in vacuo*, purification by silica gel column chromatography (gradient from pure CH_2Cl_2 to 4 % MeOH in CH_2Cl_2) afforded **4H** as a pale yellow oil (312 mg, 40 %). **^{1}H NMR** (500 MHz, $CDCl_3$) δ (ppm): 7.73 (1H, s, triazole C*H*), 7.69 (1H, t, ^3J = 7.7 Hz, pyridine Ar*H*), 7.24 (1H, d, ^3J = 7.8 Hz, pyridine Ar*H*), 7.09 (1H, d, ^3J = 7.6 Hz, pyridine Ar*H*), 5.66 (2H, s, CH_2-N triazole), 4.77 (2H, d, ^3J = 5.2 Hz, CH_2OH), 4.70 (2H, s, CH_2-C triazole), 3.53–3.71 (13H, m, TEG alkyl-CH_2 + O*H*), 3.36 (3H, s, TEG alkyl-CH_3); **^{13}C NMR** (125 MHz, $CDCl_3$) δ (ppm): 159.9, 153.2, 145.3, 137.8, 123.2, 120.6, 120.0, 71.6, 70.3, 70.3, 70.3, 70.2, 69.5, 64.4, 64.0, 58.7, 55.1; **HR-MS** (ESI +ve) *m/z*: 367.19698 ([M + H]$^+$, $C_{17}H_{27}O_5N_4$ calc. 367.19760).

TEG-appended XB 'hydroxy-arm' precursor, **4I**

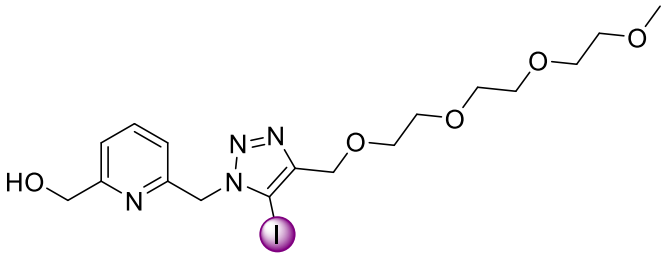

(6-(azidomethyl)pyridine-2-yl)methanol **2** (272 mg, 1.66 mmol) was dissolved in a 1:1 mixture of dry, degassed THF/CH_3CN (5 mL) and the reaction vessel covered in foil. Sodium iodide (995 mg, 6.64 mmol) and copper(II) perchlorate hexahydrate (1.23 g, 3.32 mmol) were added

and the solution stirred for 5 minutes. Further added were TBTA (17.6 mg, 0.033 mmol), DBU (252 mg, 1.66 mmol, in 0.5 mL 1:1 THF/CH_3CN) and TEG alkyne **3** (335 mg, 1.66 mmol, in 0.5 ml 1:1 THF/CH_3CN) and the mixture stirred at room temperature under a N_2 atmosphere overnight. The reaction mixture was diluted with CH_2Cl_2 (25 mL) and washed with $NH_4OH_{(aq)}$ (3 x 20 mL), brine (2 x 20 mL) and dried over $MgSO_4$. After removal of the solvent *in vacuo*, purification by silica gel column chromatography (gradient from pure CH_2Cl_2 to 3 % MeOH in CH_2Cl_2) afforded **4I** as a pale orange oil which solidified to an off-white solid upon standing overnight (522 mg, 64 %). **^{1}H NMR** (500 MHz, $CDCl_3$) δ (ppm): 7.68 (1H, t, ^3J = 7.8 Hz, pyridine Ar*H*), 7.20 (1H, d, ^3J = 7.6 Hz, pyridine Ar*H*), 6.93 (1H, d, ^3J = 7.6 Hz, pyridine Ar*H*), 5.75 (2H, s, CH_2-N iodotriazole), 4.75 (2H, d, ^3J = 5.0 Hz, CH_2OH), 4.66 (2H, s, CH_2-C iodotriazole), 3.54–3.71 (13H, m, TEG alkyl-*CH*$_2$ + O*H*), 3.37 (3H, s, TEG alkyl-*CH*$_3$); **^{13}C NMR** (125 MHz, $CDCl_3$) δ (ppm): 159.2, 152.9, 148.9, 137.8, 120.2, 119.9, 81.4, 71.9, 70.6, 70.5, 70.4, 69.7, 64.3, 63.8, 59.0, 55.2; one peak missing, presumed overlapped; **HR-MS** (ESI +ve) *m/z*: 493.09458 ([M + H]$^+$, $C_{17}H_{26}O_5N_4I$ calc. 493.09424).

TEG-appended HB ‘chloro-arm’ precursor, **5H**

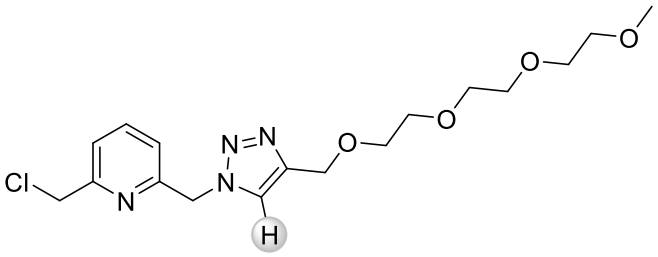

To a solution of **4H** (974 mg, 2.66 mmol) in dry CH_2Cl_2 (20 ml) at 0 °C, was slowly added $SOCl_2$ (0.29 ml, 3.99 mmol) and the reaction stirred at room temperature under a N_2 atmosphere for 6 hrs. The stirring mixture was carefully quenched and neutralised by the slow addition of a saturated $Na_2CO_{3(aq)}$ solution at 0 °C resulting in vigorous gas evolution. Thereafter, the biphasic mixture was further diluted with CH_2Cl_2 (25 ml) and washed with H_2O (2 x 25 ml). The organic layer was dried over $MgSO_4$ and the solvent removed *in vacuo*. Purification using silica gel column chromatography (gradient from pure CH_2Cl_2 to 3 % MeOH in CH_2Cl_2) afforded the chloro-arm **5H** as a clear, light orange oil (879 mg, 86 %). **^{1}H NMR** (500 MHz, $CDCl_3$) δ (ppm): 7.74 (1H, s, triazole C*H*), 7.72 (1H, t, ^3J = 7.78 Hz, pyridine Ar*H*), 7.45 (1H, d, ^3J = 7.78 Hz, pyridine Ar*H*), 7.11 (1H, d, ^3J = 7.76 Hz, pyridine Ar*H*), 5.65 (2H, s, CH_2-N triazole), 4.70 (2H, s, CH_2-C triazole), 4.66 (2H, s, CH_2Cl), 3.53–3.71 (12H, m, TEG alkyl-*CH*$_2$), 3.37 (3H, s, TEG alkyl-*CH*$_3$); **^{13}C NMR** (125 MHz, $CDCl_3$) δ (ppm): 156.7, 154.1, 145.6, 138.3, 123.2, 122.3, 121.4, 71.8, 70.5, 70.4, 70.4, 70.4, 69.6, 64.6, 58.9, 55.2, 46.2; **HR-MS** (ESI +ve) *m/z*: 385.16367 ([M + H]$^+$, $C_{17}H_{26}N_4O_4Cl$ calc. 385.16371).

TEG-appended XB ‘chloro-arm’ precursor, **5I**

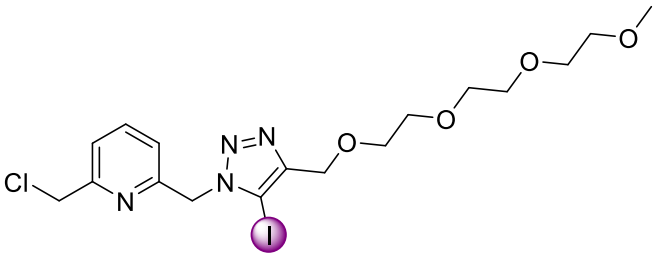

To a solution of **4I** (1.42 g, 2.88 mmol) in dry CH_2Cl_2 (25 ml) at 0 °C, was slowly added $SOCl_2$ (0.32 ml, 4.32 mmol) and the reaction stirred at room temperature under a N_2 atmosphere for 6 hrs. The stirring mixture was carefully quenched and neutralised by the slow addition of a saturated $Na_2CO_{3(aq)}$ solution at 0 °C resulting in vigorous gas evolution. Thereafter, the biphasic mixture was further diluted with CH_2Cl_2 (25 ml) and washed with H_2O (2 x 25 ml). The organic layer was dried over $MgSO_4$ and the solvent removed *in vacuo*. Purification using silica gel column chromatography (gradient from pure CH_2Cl_2 to 3 % MeOH in CH_2Cl_2) afforded the chloro-arm **5I** as a clear, amber oil (1.19 g, 81 %). **^{1}H NMR** (500 MHz, $CDCl_3$) δ (ppm): 7.70 (1H, t, ^3J = 7.8 Hz, pyridine Ar*H*), 7.44 (1H, d, ^3J = 7.8 Hz, pyridine Ar*H*), 6.85 (1H, d, ^3J = 7.8 Hz, pyridine Ar*H*), 5.74 (2H, s, CH_2-N iodotriazole), 4.67 (2H, s, CH_2-C iodotriazole), 4.66 (2H, s, CH_2Cl), 3.55–3.71 (12H, m, TEG alkyl-CH_2), 3.38 (3H, s, TEG alkyl-CH_3); **^{13}C NMR** (125 MHz, $CDCl_3$) δ (ppm): 156.6, 153.8, 148.9, 138.2, 122.1, 120.6, 81.4, 71.9, 70.5, 70.5, 70.4, 69.7, 64.2, 59.0, 55.3, 46.3, one peak missing, presumed overlapped; **HR-MS** (ESI +ve) *m/z*: 533.04289 ([M + Na]$^+$, $C_{17}H_{24}N_4O_4ClINa$ calc. 533.04230).

Tris(TEG)-appended HB tripodal ligand, **6H**

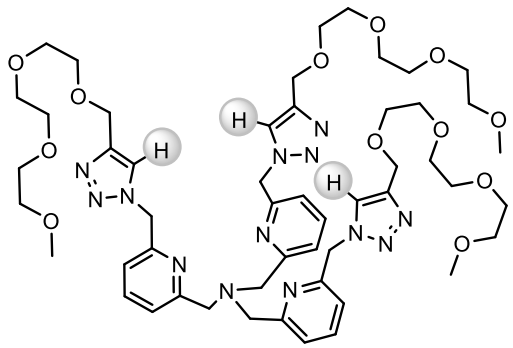

To a solution of **5H** (825 mg, 2.14 mmol) fully dissolved in dry CH_3CN (30 mL) was added NH_4OAc (3.30 g, 42.8 mmol), Na_2CO_3 (4.54 g, 42.8 mmol) and KI (356 mg, 2.14 mmol) as solid portions. The reaction flask was completely sealed, and the mixture vigorously stirred for two days at room temperature after which no evidence of **5H** was observed by TLC or ESI-

MS analyses. Thereafter, the creamy off-white suspension was directly transferred to a separating funnel and *ca.* 20 ml H_2O very gently pipetted into the vessel. The cloudy, lower aqueous layer was separated, and the remaining clear pale yellow organic layer concentrated *in vacuo*. The resultant crude residue was redissolved in $CHCl_3$ (50 mL) and washed with water (2 x 20 mL) and the organics dried over $MgSO_4$. Solvent removal and purification by preparative thin layer chromatography (5 % MeOH in $CHCl_3$) afforded the tripodal ligand **6H** as a deep yellow oil (501 mg, 66 % yield). **^{1}H NMR** (500 MHz, $CDCl_3$) δ (ppm): 7.73 (3H, s, triazole C*H*), 7.64 (3H, t, ^3J = 7.7 Hz, pyridine Ar*H*), 7.46 (3H, d, ^3J = 7.6 Hz, pyridine Ar*H*), 7.01 (3H, d, ^3J = 7.6 Hz, pyridine Ar*H*), 5.62 (6H, s, CH_2-N triazole), 4.68 (6H, s, CH_2-C triazole), 3.86 (6H, s, CH_2-N tertiary amine), 3.53–3.70 (36 H, m, TEG alkyl-CH_2), 3.36 (9H, s, TEG alkyl-CH_3); **^{13}C NMR** (125 MHz, $CDCl_3$) δ (ppm): 159.4, 153.8, 145.5, 137.7, 123.2, 122.4, 120.5, 71.9, 70.5, 70.5, 70.4, 69.7, 64.6, 59.9, 59.0, 55.5, one peak missing, presumed overlapped. **HR-MS** (ESI +ve) *m/z*: 1062.5746 ([M + H]$^+$, $C_{51}H_{76}N_{13}O_{12}$ calc.1062.5736).

Tris(TEG)-appended XB tripodal ligand, **6I**

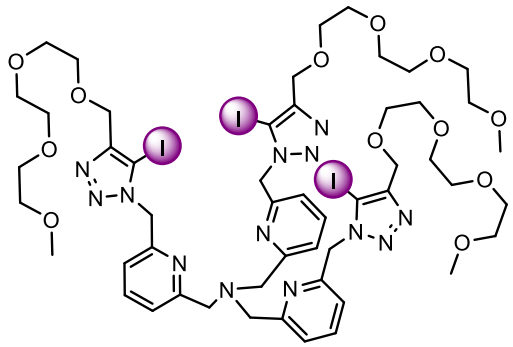

To a solution of **5I** (882 mg, 1.73 mmol) fully dissolved in dry CH_3CN (30 mL) was added NH_4OAc (2.67 g, 34.6 mmol), Na_2CO_3 (3.67 g, 34.6 mmol) and KI (287 mg, 1.73 mmol) as solid portions. The reaction flask was completely sealed, and the mixture vigorously stirred for two days at room temperature after which no evidence of **5I** was observed by TLC or ESI-MS analyses. Thereafter, the creamy off-white suspension was directly transferred to a separating funnel and *ca.* 20 ml H_2O very gently pipetted into the vessel. The cloudy, lower aqueous layer was separated, and the remaining clear, light yellow organic layer concentrated *in vacuo*. The resultant crude residue was redissolved in $CHCl_3$ (50 mL) and washed with water (2 x 20 mL) and the organics dried over $MgSO_4$. Solvent removal and purification by preparative thin layer chromatography (6 % MeOH in CH_2Cl_2) afforded the tripodal ligand **6I** as a dark yellow oil (497 mg, 60 % yield). **^{1}H NMR** (500 MHz, $CDCl_3$) δ (ppm): 7.63 (3H, t, ^3J = 7.7 Hz, pyridine Ar*H*), 7.43 (3H, d, ^3J = 7.6 Hz, pyridine Ar*H*), 6.79 (3H, d, ^3J = 7.0 Hz, pyridine Ar*H*), 5.72 (6H, s, CH_2-N iodotriazole), 4.64 (6H, s, CH_2-C iodotriazole), 3.84 (6H, s, CH_2-N tertiary amine), 3.53–

3.68 (36H, m, TEG alkyl-CH_3), 3.37 (9H, s, TEG-alkyl CH_3); **^{13}C NMR** (125 MHz, $CDCl_3$) δ (ppm): 159.4, 153.4, 148.8, 137.6, 122.4, 119.7, 81.5, 71.9, 70.6, 70.5, 70.4, 69.7, 64.3, 59.6, 59.0, 55.5, one peak missing, presumed overlapped; **HR-MS** (ESI +ve) *m/z*: 1440.2665 ([M + H]$^+$, $C_{51}H_{73}N_{13}O_{12}I_3$ calc. 1440.2635).

Succinimidyl-3-propiolate, **7**[4]

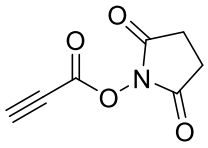

This literature compound was prepared according to modified procedures. To a stirring solution of propiolic acid (0.5 mL, 8 mmol) in dry acetonitrile (50 mL) at 0 °C was added *N*-hydroxysuccinimide (0.92 g, 8 mmol). Separately, dicyclohexylcarbodiimide (DCC) (1.65 g, 8 mmol) was added portion wise to the reaction mixture, which was kept stirring for 8 hours at 4 °C under N_2. After filtration of the white precipitate under gravity, removal of the solvent *in vacuo* gave the activated ester **7** in excellent purity as a pale yellow oil, which solidified to a crystalline solid upon standing for 1 – 2 hours at room temperature (909 mg, 68 %). *(N.B. due to the unstable nature of the compound, the obtained solid was stored in a vial at -20 °C until further used).* **^{1}H NMR** (500 MHz, $CDCl_3$) *δ* (ppm): 3.34 (1H, s, C≡C*H*), 2.86 (4H, s, COCH_2); **^{13}C NMR** (125 MHz, $CDCl_3$) *δ* (ppm): 168.2, 147.7, 82.1, 70.1, 25.5; **LR-MS** (ESI +ve) *m/z*: not observed.

N.B. For all of the β-cyclodextrin precursor compounds leading up to the synthesis of the key permethylated β-cyclodextrin (pmβCD) alkyne **9**[5] (see Scheme 2, main paper), all mono-functionalisation procedures were carried out at the 6- position on the narrow rim of the truncated cone as shown in Figure S1. Therefore, this numbering system is also used for the assignment of the relevant ^{1}H NMR signals in the following characterisation data of the novel pmβCD compounds **10** – **12l** leading to the synthesis of the tris(pmβCD)-appended XB tripod **13l**·2OTf**.**

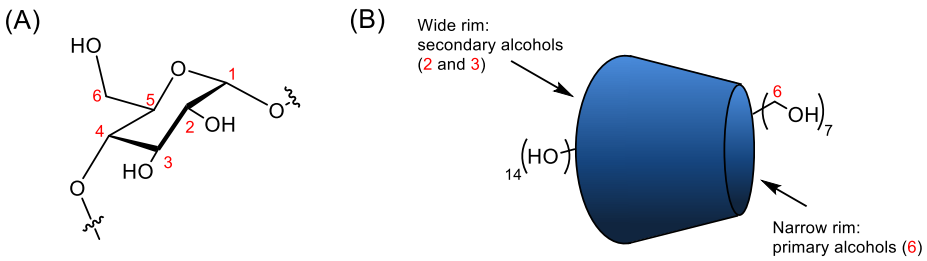

Figure S1. (A) Numbering scheme for the glucopyranose units of the β-CD cone and (B) distribution of the primary and secondary alcohol moieties on its narrow and wide rims, respectively.

It should be further noted that by convention, in a mono-substituted β-CD derivative, the functionalised glucopyranose unit is denoted A, with the remaining units labelled B-G. 6^{A}-substituted therefore means that Carbon 6 of glucopyranose unit A is functionalised.

6^{A}-amido-pmβCD alkyne, **9**

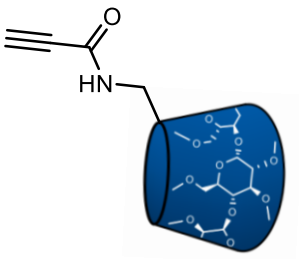

To a solution of succinimidyl-3-propiolate **7**[4] (82.3 mg, 0.494 mmol) and permethylated β-cyclodextrin amine **8**[6] (500 mg, 0.353 mmol) in dry CH_2Cl_2 was added 4-dimethylaminopyridine (DMAP) (10 mg, 0.08 mmol). The mixture was left to stir at room temperature under a N_2 atmosphere overnight, after which no evidence of the permethylated β-cyclodextrin amine was observed by TLC or ESI-MS. After removal of the solvent *in vacuo*, purification by silica gel

column chromatography (4 % MeOH in EtOAc) afforded **9** as a crystalline white solid (362 mg, 70 %). **^{1}H NMR** (500 MHz, $CDCl_3$) δ (ppm): 6.74 (1H, t, ^{3}J = 5.9 Hz, amide N*H*), 5.08–5.18 (7H, m, β-CD H_1), 3.17–4.08 (102H, m, β-CD $H_{2\text{-}6}$ + CH_3O), 2.84 (1H, s, C≡C*H*); **^{13}C NMR** (125 MHz, $CDCl_3$) δ (ppm): 152.2, β-CD signals consistent with loss of C7 symmetry: (99.2–98.6; *β*-CD C_1), 82.1–81.3, 80.6–79.8, 77.7, 73.0, 71.5–70.1, 61.6–61.2, 59.5–58.3; **HR-MS** (ESI +ve) *m/z*: 1488.67853 ([M + Na]$^+$, $C_{65}H_{111}NO_{35}Na$ calc. 1488.68288).

6^{A}-amido-pmβCD-appended XB ‘hydroxy-arm’ precursor, **10I**

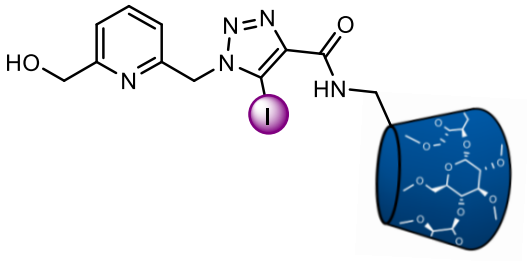

(6-(azidomethyl)pyridine-2-yl)methanol **2** (41 mg, 0.25 mmol) was dissolved in a 1:1 mixture of dry, degassed THF/CH_3CN (2 mL) and the reaction vessel covered in foil. Sodium iodide (149 mg, 1.00 mmol) and copper(II) perchlorate hexahydrate (185 mg, 0.5 mmol) were added and the solution stirred for 5 minutes. Further added were DBU (37.3 µL, 0.25 mmol) and pm*β*CD alkyne **9** (366 mg, 0.25 mmol) and the mixture stirred at room temperature under a N_2 atmosphere overnight. The reaction mixture was diluted with $CHCl_3$ (25 mL) and washed with $NH_4OH_{(aq)}$ (3 x 20 mL), brine (2 x 20 mL) and dried over $MgSO_4$. After removal of the solvent *in vacuo*, purification by silica gel column chromatography (gradient from pure $CHCl_3$ to 3 % MeOH in $CHCl_3$) afforded the arm precursor **10I** as a crystalline off-white solid (232 mg, 53 %). **^{1}H NMR** (500 MHz, $CDCl_3$) δ (ppm): 7.70 (1H, t, ^{3}J = 7.8 Hz, pyridine Ar*H*), 7.47 (1H, t, ^{3}J = 5.8 Hz, amide N*H*), 7.23 (1H, d, ^{3}J = 7.8 Hz, pyridine Ar*H*), 6.93 (1H, d, ^{3}J = 7.6 Hz, pyridine Ar*H*), 5.79 (2H, ABquart., $\Delta\delta_{AB}$ = 0.04, $^{2}J_{AB}$ = 15.5 Hz, CH_2-N iodotriazole), 5.12–5.23 (7H, m, β-CD H_1), 4.74 (2H, d, ^{3}J = 4.9 Hz, CH_2OH), 3.18–3.99 (103H, m, β-CD $H_{2\text{-}6}$ + CH_3O + O*H*); **^{13}C NMR** (125 MHz, $CDCl_3$) δ (ppm): 159.6, 159.4, 152.4, 143.3, 137.9, 120.2, β-CD signals consistent with loss of C7 symmetry: (99.2–98.5; β-CD C_1), 82.1–81.4, 80.4–79.9, 71.5–70.9, 70.1, 63.8, 61.6– 61.3, 59.2–58.3, 55.1, 39.9; **HR-MS** (ESI +ve) *m/z*: 1778.64524 ([M + Na]$^+$, $C_{72}H_{118}O_{36}N_5INa$ calc. 1778.64934).

6^{A}-amido-pmβCD-appended XB ‘chloro-arm’ precursor, **11I**

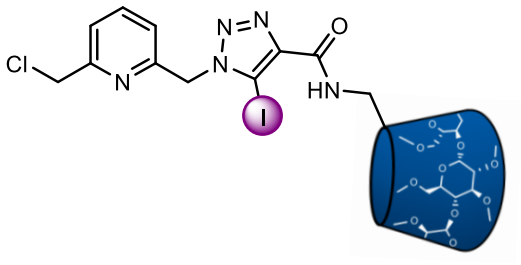

To a solution of **10I** (1.04 g, 0.59 mmol) in dry CH_2Cl_2 (25 ml) at 0 °C, was slowly added $SOCl_2$ (0.13 ml, 1.77 mmol) and the reaction stirred at rt under a N_2 atmosphere for 6 hrs. The stirring mixture was carefully quenched and neutralised by the slow addition of a saturated $Na_2CO_{3(aq)}$ solution at 0 °C resulting in vigorous gas evolution. Thereafter, the biphasic mixture was further diluted with $CHCl_3$ (25 ml) and washed with H_2O (2 x 25 ml). The organic layer was dried over $MgSO_4$ and solvent removal *in vacuo* gave the chloro-arm **11I** as a cream-coloured powder in good purity which was used without further purification (809 mg, 77 %). **^{1}H NMR** (500 MHz, $CDCl_3$) δ (ppm): 7.72 (1H, t, ^{3}J = 7.8 Hz, pyridine Ar*H*), 7.45–7.49 (2H, m, pyridine Ar*H* + amide N*H*), 6.87 (1H, d, ^{3}J = 7.8 Hz, pyridine Ar*H*), 5.78 (2H, ABquart., $\Delta\delta_{AB}$ = 0.05, $^{2}J_{AB}$ = 16.0 Hz, CH_2-N iodotriazole), 5.12–5.23 (7H, m, β-CD H_1), 4.64 (2H, s, CH_2Cl), 3.18–4.01 (102H, m, β-CD $H_{2\text{-}6}$ + CH_3O); **^{13}C NMR** (125 MHz, $CDCl_3$) δ (ppm): 159.4, 157.0, 153.3, 143.3, 138.2, 122.3, 120.5, β-CD signals consistent with loss of C7 symmetry: (99.2–98.6; β-CD C_1), 82.2–81.7, 81.4, 80.4–80.0, 71.5 – 70.9, 70.1, 61.6 – 61.3, 59.2 – 58.3, 55.2, 46.2, 39.9; **HR-MS** (ESI +ve) *m/z*: 1796.61119 ([M + Na]$^{+}$, $C_{72}H_{117}O_{35}N_5ClINa$ calc. 1796.61545).

Tris(6^A-amido-pmβCD)-appended XB tripodal ligand, **12I**

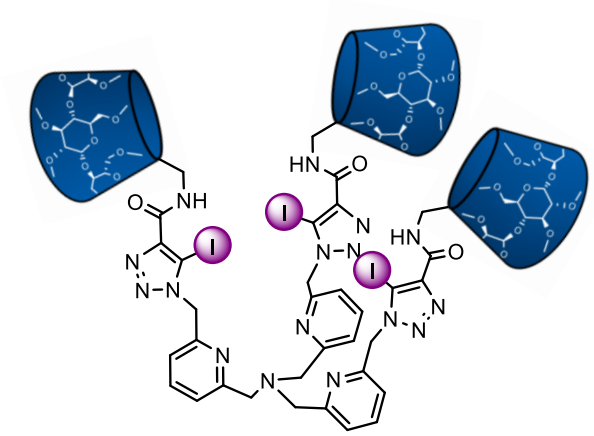

To a solution of **11I** (423 mg, 0.238 mmol) fully dissolved in dry CH_3CN (20 mL) was added NH_4OAc (550 mg, 7.14 mmol), Na_2CO_3 (757 mg, 7.14 mmol) and KI (39.5 mg, 0.238 mmol) as solid portions. The reaction flask was completely sealed, and the mixture vigorously stirred for two days at room temperature after which no evidence of **11I** was observed by TLC or ESI-MS analyses. Thereafter, the creamy white suspension was directly transferred to a separating funnel and *ca.* 5-10 ml H_2O very gently pipetted into the vessel. The cloudy, lower aqueous layer was separated, and the remaining clear pale yellow organic layer concentrated *in vacuo*. The resultant crude residue was redissolved in $CHCl_3$ (25 mL) and washed with brine (2 x 10 mL) and the organics dried over $MgSO_4$. Solvent removal and purification by preparative thin layer chromatography (6 % MeOH in CH_2Cl_2) afforded the tripodal ligand **12I** as a crystalline off-white solid upon drying *in vacuo* (216 mg, 52 % yield). **^{1}H NMR** (500 MHz, $CDCl_3$) δ (ppm): 7.66 (3H, t, ^3J = 7.7 Hz, pyridine Ar*H*), 7.46–7.49 (6H, m, pyridine Ar*H* + amide N*H*), 6.73 (3H, d, ^3J = 7.8 Hz, pyridine Ar*H*), 5.77 (6H, ABquart., $\Delta\delta_{AB}$ = 0.05, $^2J_{AB}$ = 16.1 Hz, CH_2-N iodotriazole), 5.13–5.23 (21H, m, β-CD H_1), 3.17–3.97 (312H, m, β-CD $H_{2\text{-}6}$ + CH_3O + CH_2-N tertiary amine); **^{13}C NMR** (125 MHz, $CDCl_3$) δ (ppm): 159.5, 153.1, 143.3, 137.7, 122.3, 119.5, β-CD signals consistent with loss of C7 symmetry: (99.0–98.6; β-CD C_1), 82.3–81.2, 80.4–79.9, 71.5–70.0, 61.5–61.4, 59.7–58.4, 55.5, 39.8; **HR-MS** (ESI +ve) *m/z*: 2627.98525 ([M + H + Na]$^{2+}$, $C_{216}H_{352}O_{105}N_{16}I_3Na$ calc. 2627.98919).

Tris(pmβCD)-appended XB Cu(II) tripod, **13I**·2OTf

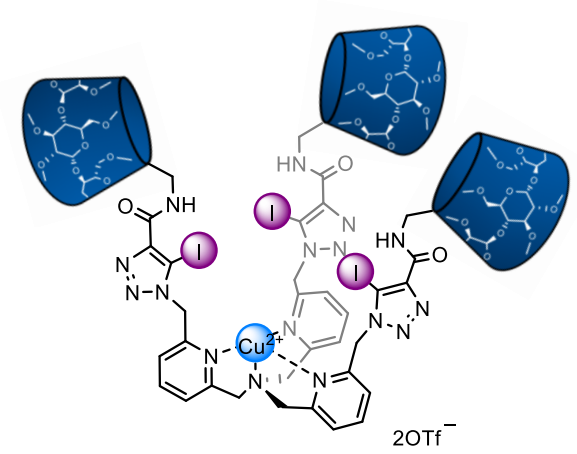

To tripodal ligand **12I** (100 mg, 0.02 mmol) in a 1:1 mixture of CH_2Cl_2/MeOH (6 mL) was added copper(II) trifluoromethansulfonate (7.23 mg, 0.02 mmol) and the solution stirred at room temperature under a N_2 atmosphere for 3 hours. After removal of the solvent *in vacuo*, the resultant deep blue residue was triturated with ice cold Et_2O (*ca*. 5 mL). The ethereal layer was carefully decanted with a pipette and the contents of the flask dried under high vacuum to afford metallo-tripodal receptor **13I**·2OTf as a fine, pale blue crystalline powder (106 mg, quantitative). **UV-vis** (CH_3CN/ H_2O 6:4 *v/v*, 10 mM HEPES, λ_{max}/ nm, (ε/ M^{-1} cm^{-1})): 645 (182), 770 (119); **EPR** (CH_3CN/ H_2O 6:4 *v/v*, 10 mM HEPES, 105 K): $g\|$ = 2.225, $g\perp$ = 2.065, $A\|_1$ = 185.0 x 10^{-4} cm^{-1}, $A\|_2$ = 220.0 x 10^{-4} cm^{-1}; **HR-MS** (ESI +ve) *m/z*: 2647.46450 ($[M - 2OTf]^{2+}$, $C_{216}H_{351}N_{16}O_{105}I_3{}^{63}Cu$ calc. 2647.45519).

Tetrabutylammonium salt of pinacolyl methylphosphonic acid, **TBA PMP**

To a chilled solution of 1.0 eqv of a methanolic solution of tetrabutylammonium (TBA) hydroxide at 0 °C directly was added 1.0 eqv of neutral pinacolyl methylphoshonic acid over 5 minutes. The resulting reaction mixture was allowed to warm to room temperature and stirred for 3 hours. The appropriate TBA pinacolyl methyl phosphonate salt was obtained by removal of the solvent *in vacuo* and leaving the salt to dry under high vacuum for at least 5 days. The resultant salt was obtained a white powder and stored in a vacuum desiccator with P_2O_5 desiccant at room temperature.

S3. Characterisation Data

S3.1 ^{1}H, ^{13}C NMR and HR-MS of all novel compounds

2,5,8,11-tetraoxatetradec-13-yne, 3

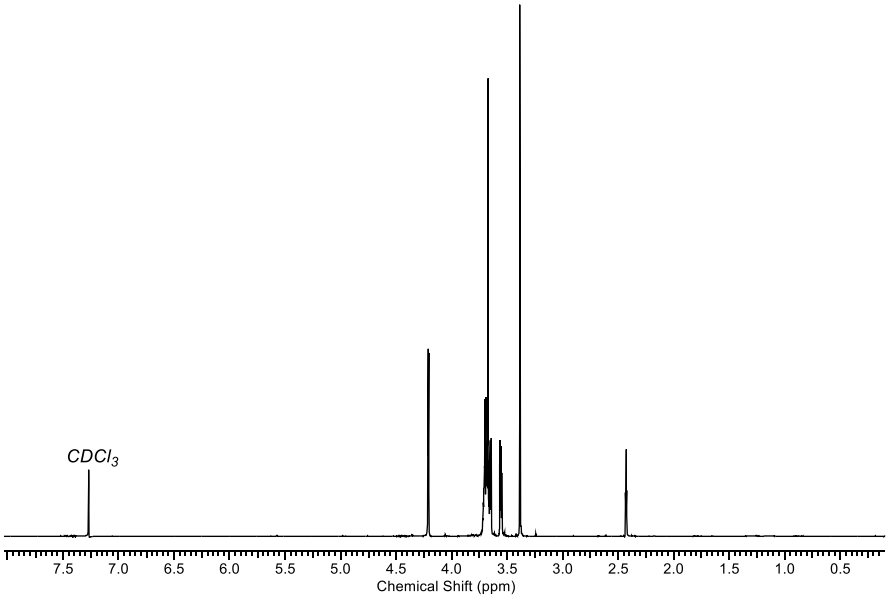

Figure S2. ^{1}H NMR of alkyne **3** in $CDCl_3$ (500 MHz, *T* = 298 K).

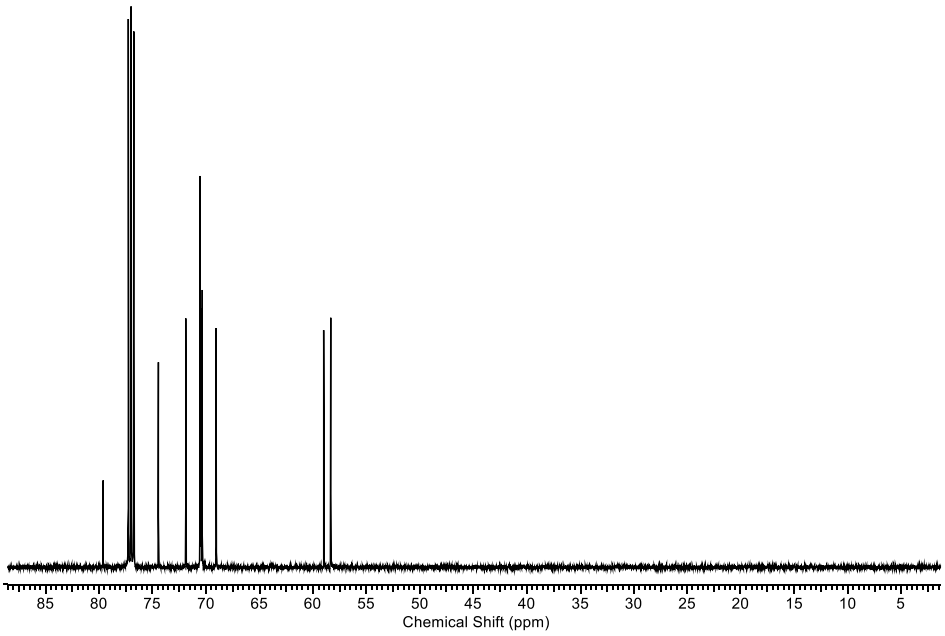

Figure S3. ^{13}C NMR of alkyne **3** in $CDCl_3$ (125 MHz, *T* = 298 K).

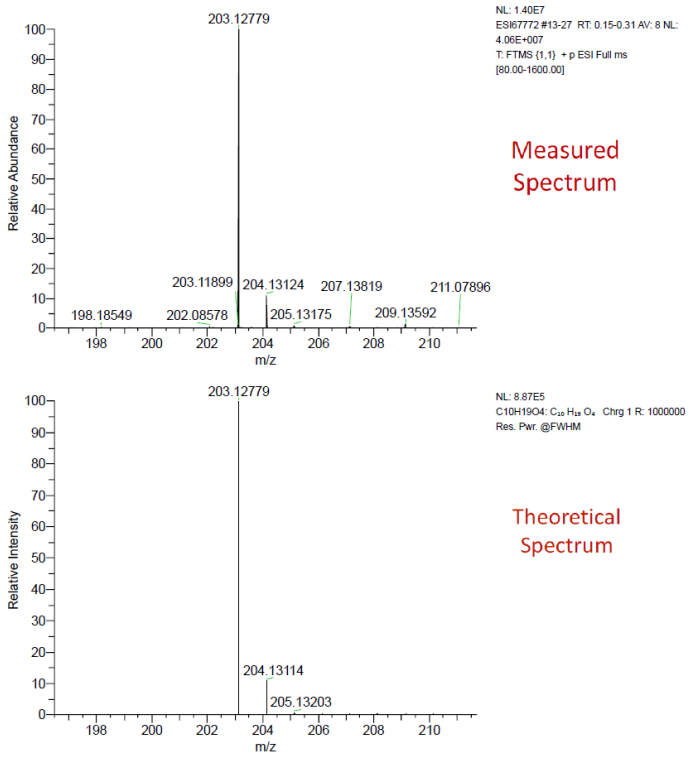

Figure S4. High-resolution mass spectrum of alkyne **3**.

TEG-appended HB 'hydroxy-arm' precursor, 4H

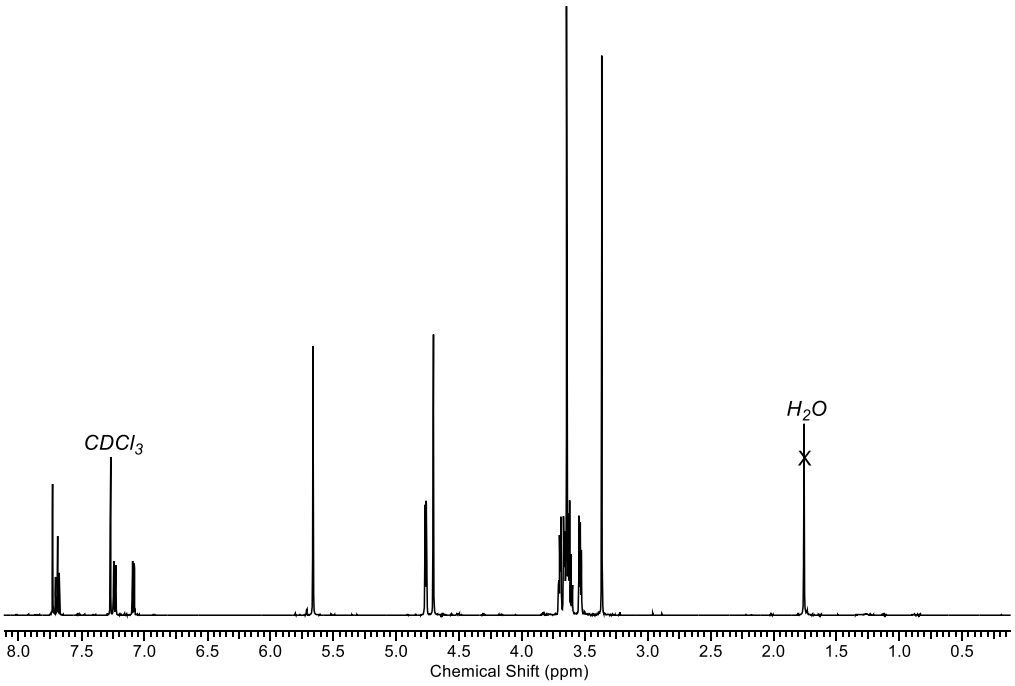

Figure S5. ^{1}H NMR of precursor **4H** in $CDCl_3$ (500 MHz, T = 298 K).

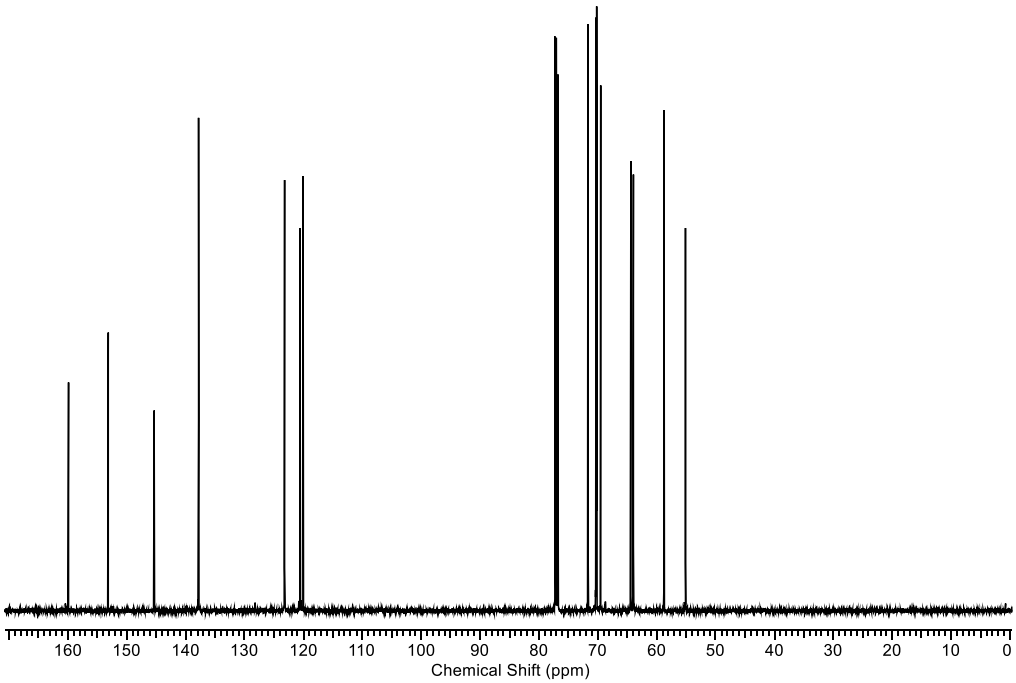

Figure S6. ^{13}C NMR of precursor **4H** in $CDCl_3$ (125 MHz, *T* = 298 K).

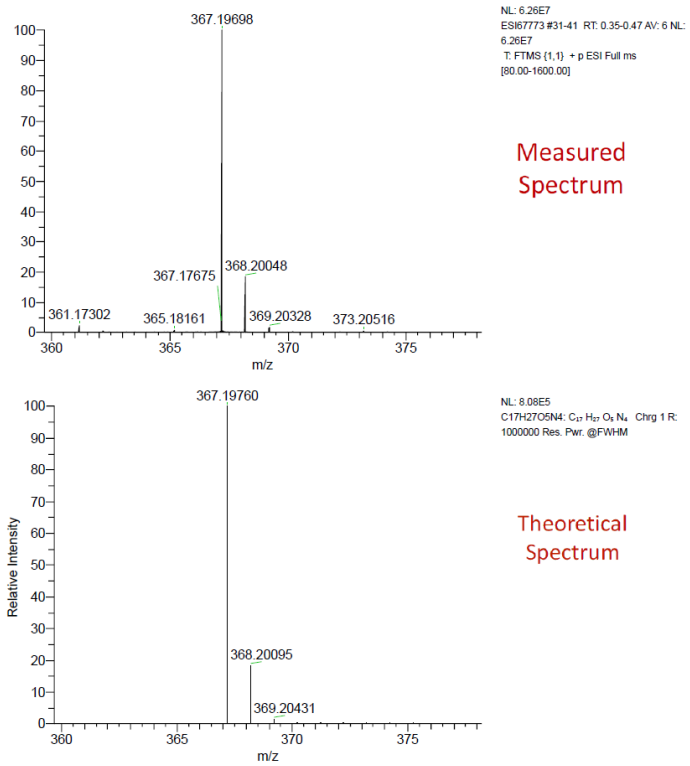

Figure S7. High-resolution mass spectrum of precursor **4H**.

TEG-appended XB 'hydroxy-arm' precursor, 4l

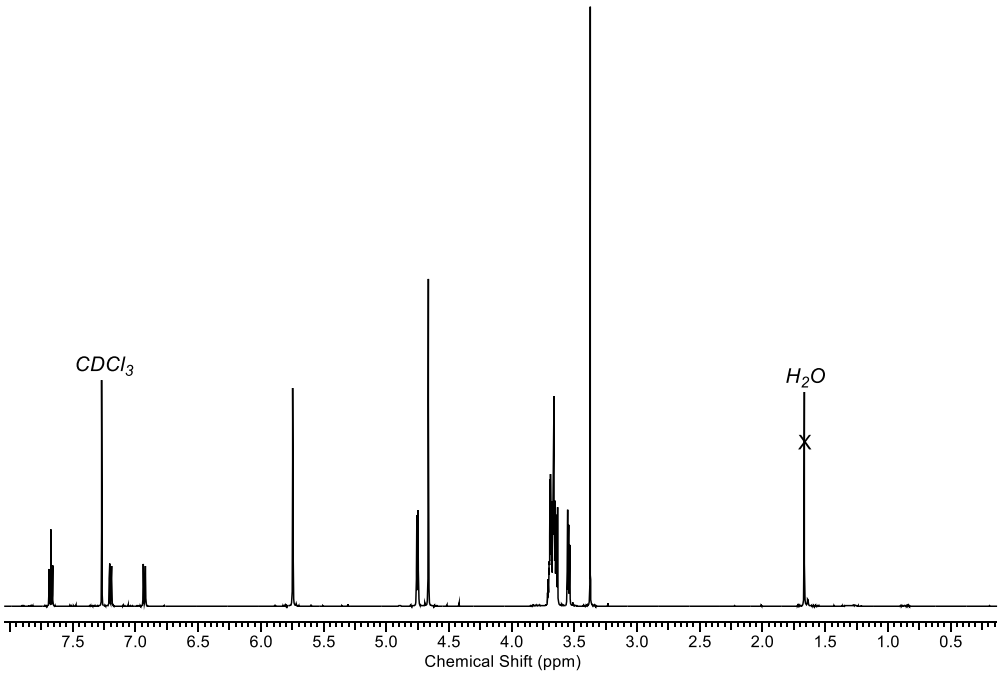

Figure S8. ^{1}H NMR of precursor **4l** in $CDCl_3$ (500 MHz, *T* = 298 K).

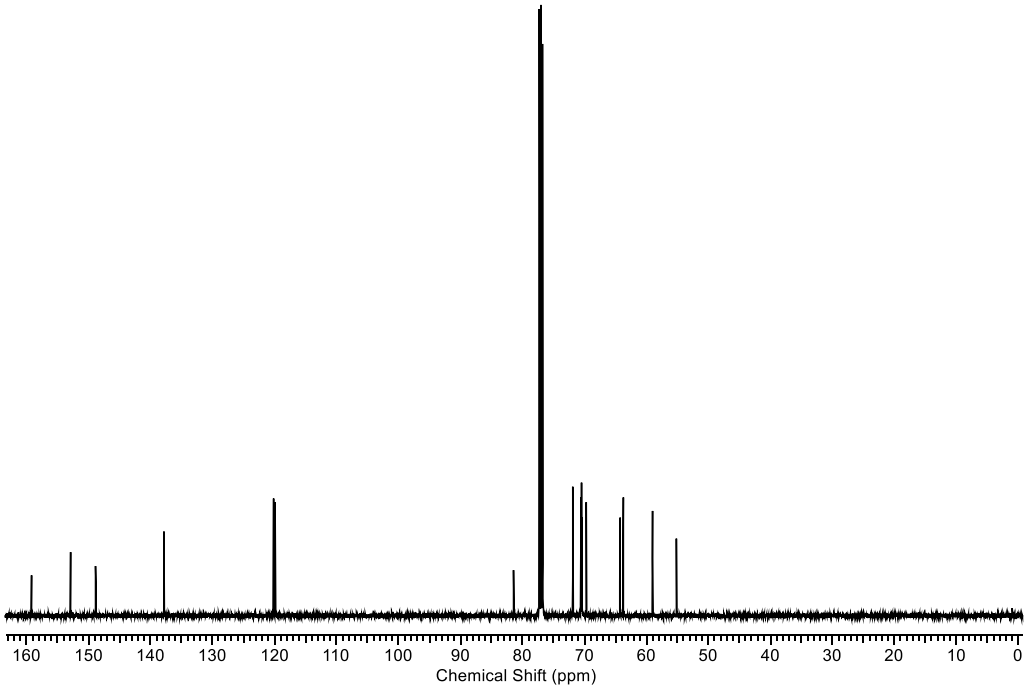

Figure S9. ^{13}C NMR of precursor **4l** in $CDCl_3$ (125 MHz, *T* = 298 K).

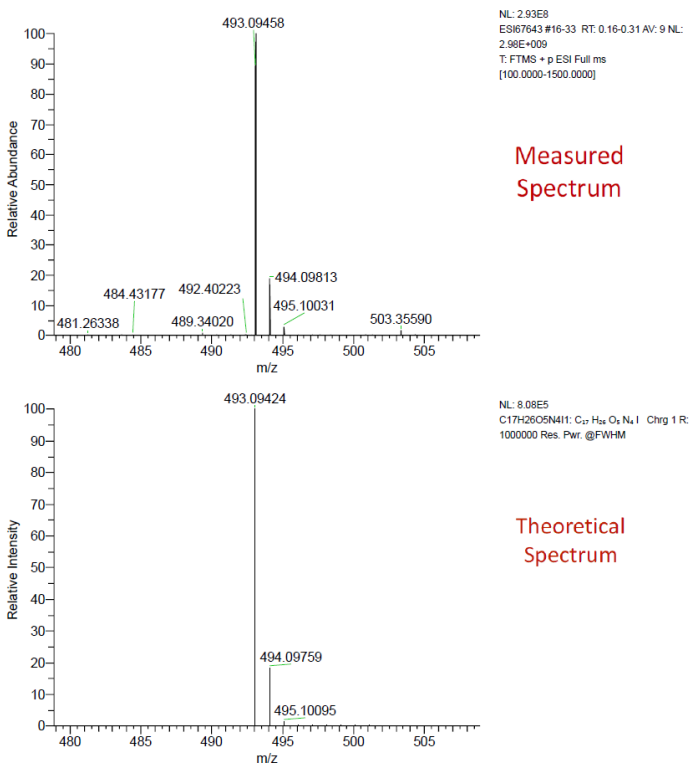

Figure S10. High-resolution mass spectrum of precursor **4I**.

TEG-appended HB 'chloro-arm' precursor, 5H

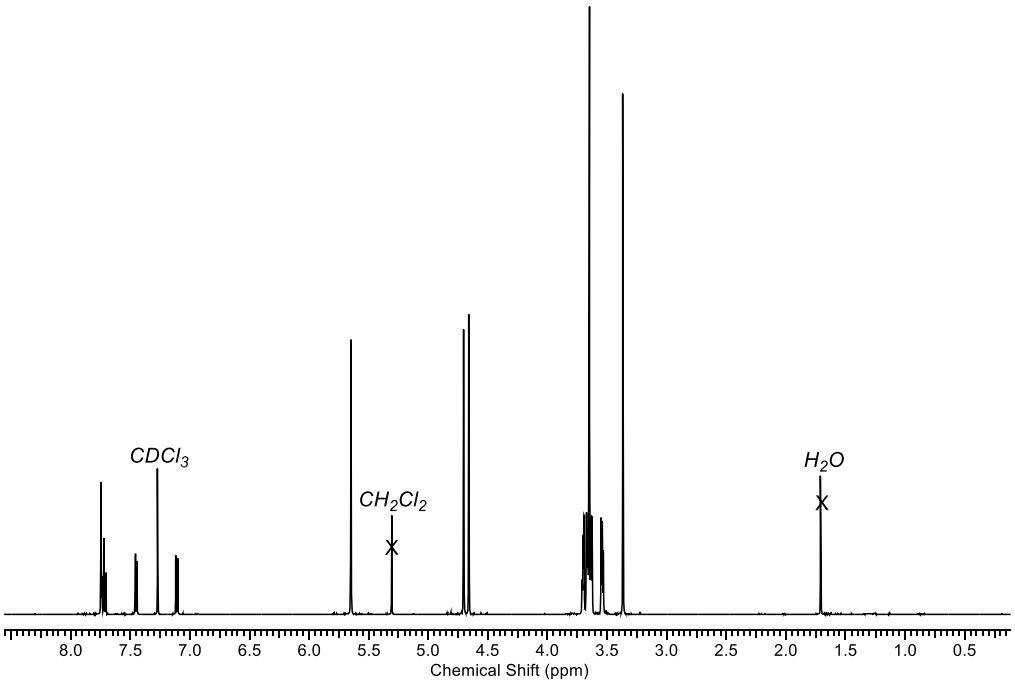

Figure S11. ^{1}H NMR of precursor **5H** in $CDCl_3$ (500 MHz, T = 298 K).

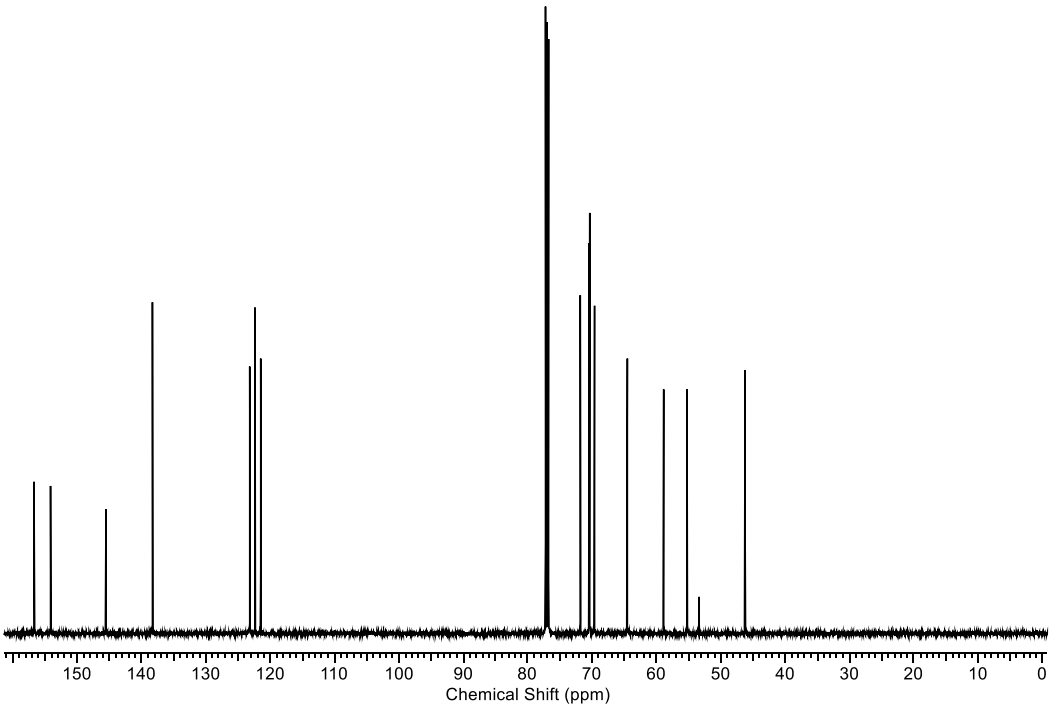

Figure S12. ^{13}C NMR of precursor **5H** in $CDCl_3$ (125 MHz, *T* = 298 K).

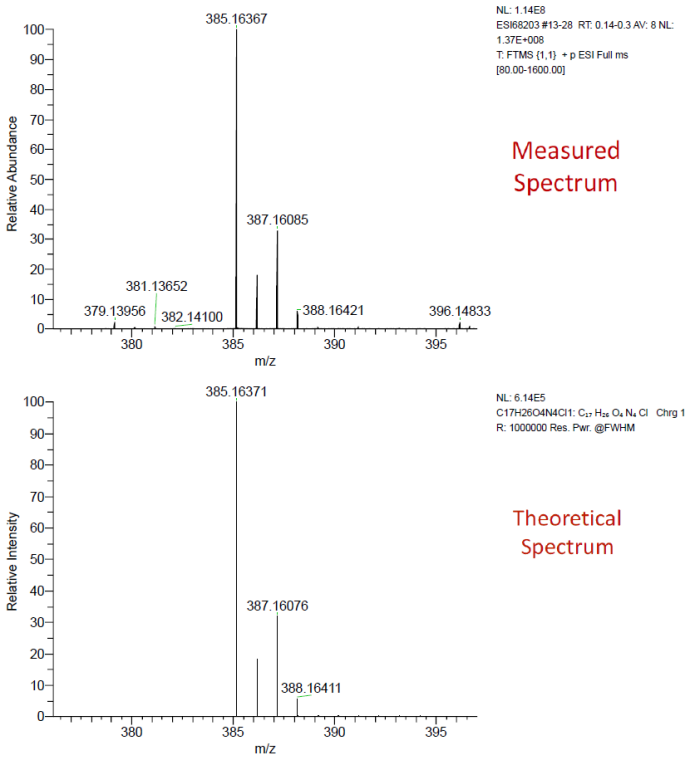

Figure S13. High-resolution mass spectrum of precursor **5H**.

TEG-appended XB ‘chloro-arm’ precursor, 5I

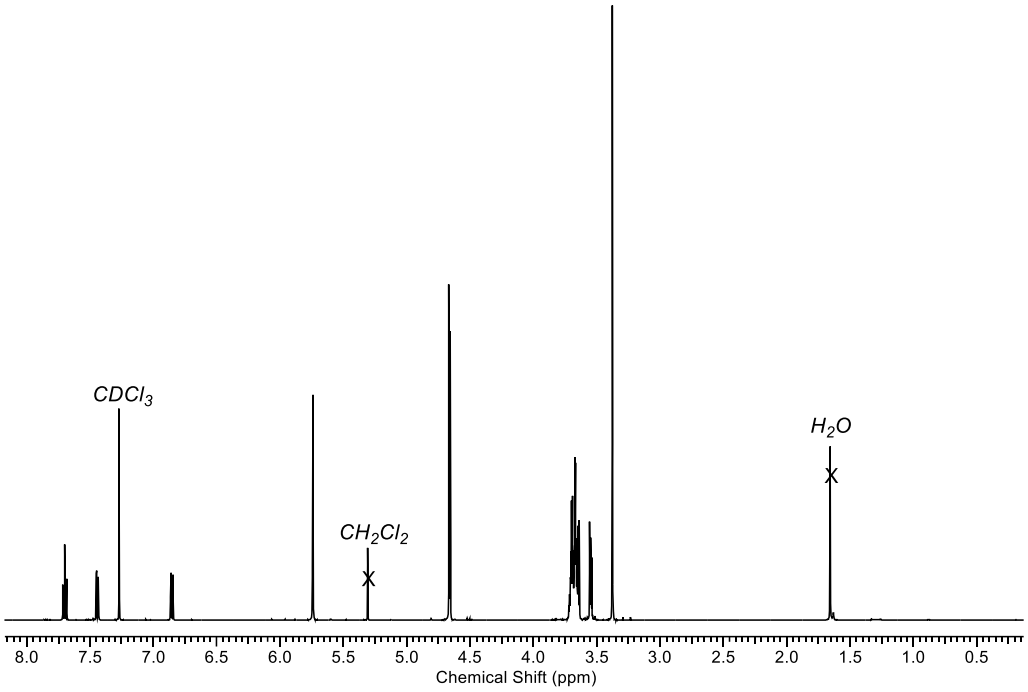

Figure S14. ^{1}H NMR of precursor **5I** in $CDCl_3$ (500 MHz, *T* = 298 K).

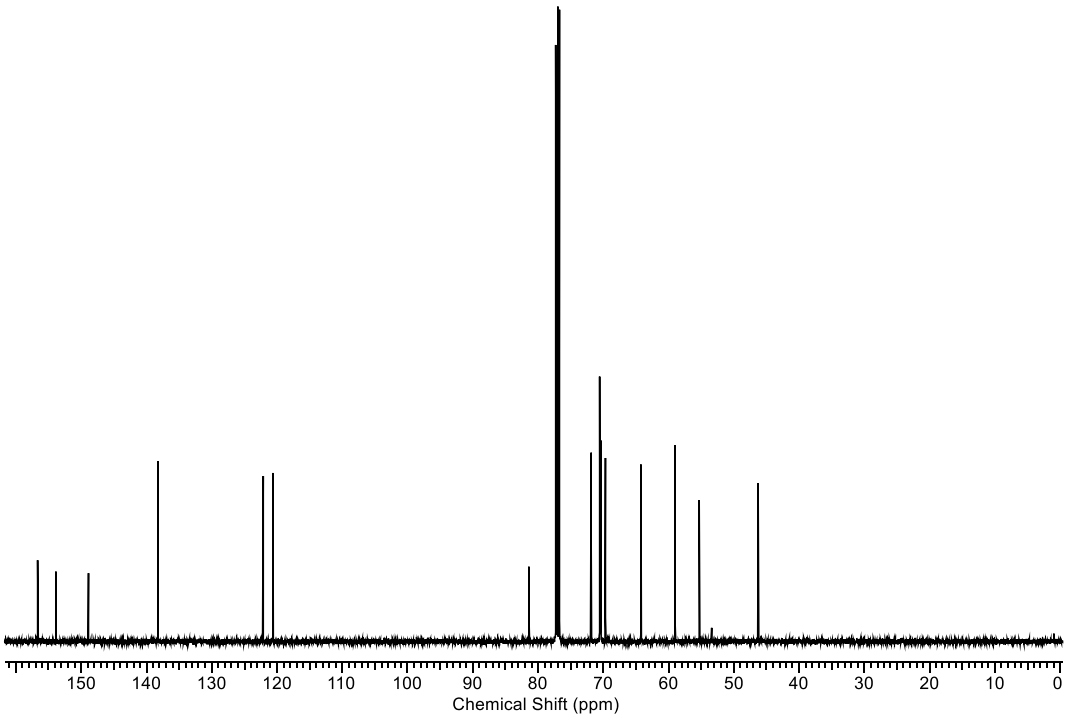

Figure S15. ^{13}C NMR of precursor **5I** in $CDCl_3$ (125 MHz, *T* = 298 K).

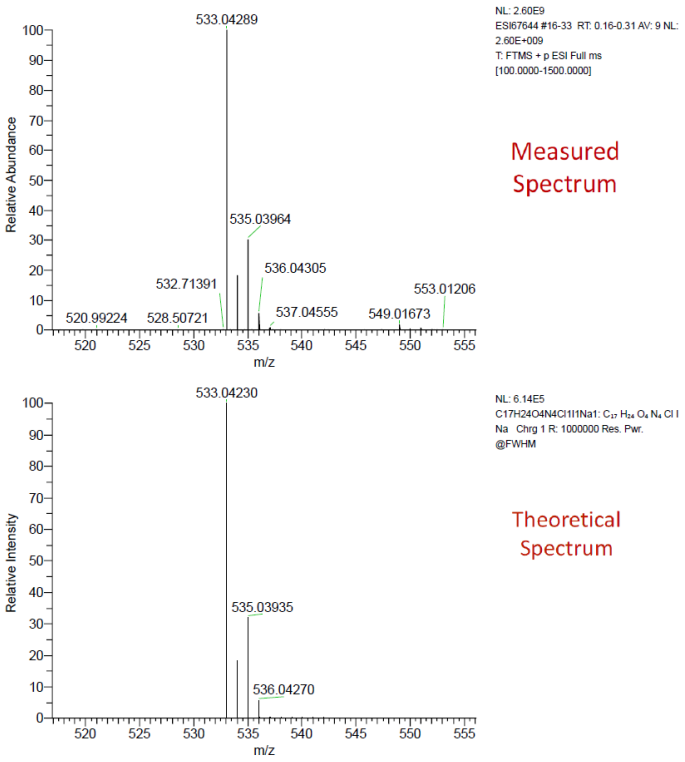

Figure S16. High-resolution mass spectrum of precursor **5I**.

Tripodal HB ligand, 6H

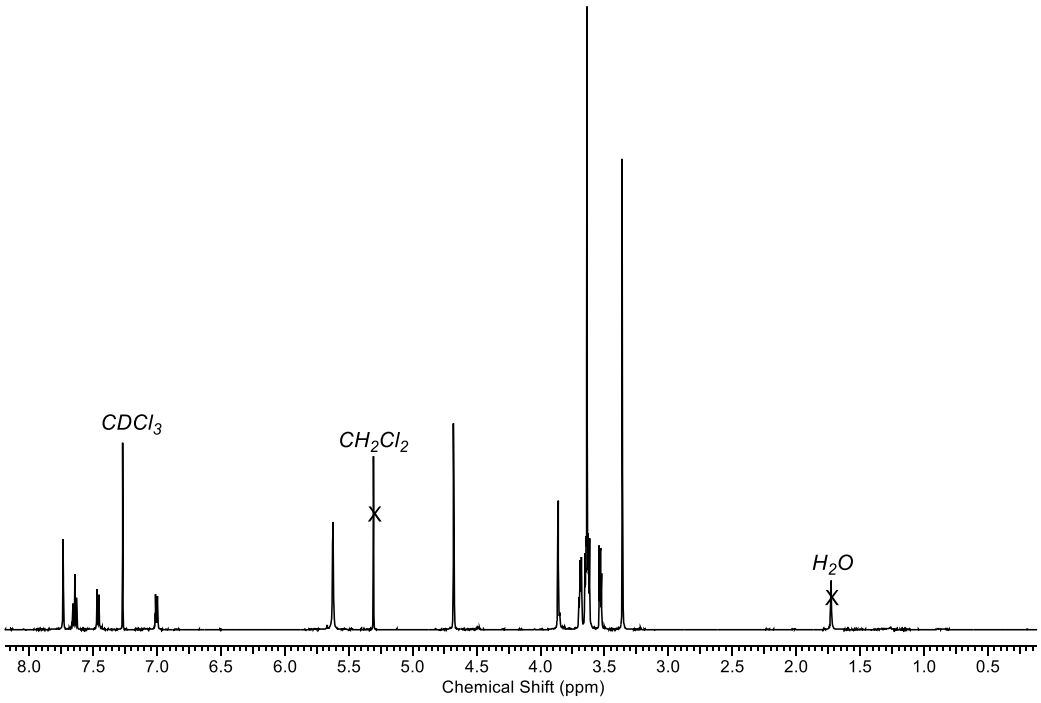

Figure S17. ^{1}H NMR of ligand **6H** in $CDCl_3$ (500 MHz, T = 298 K).

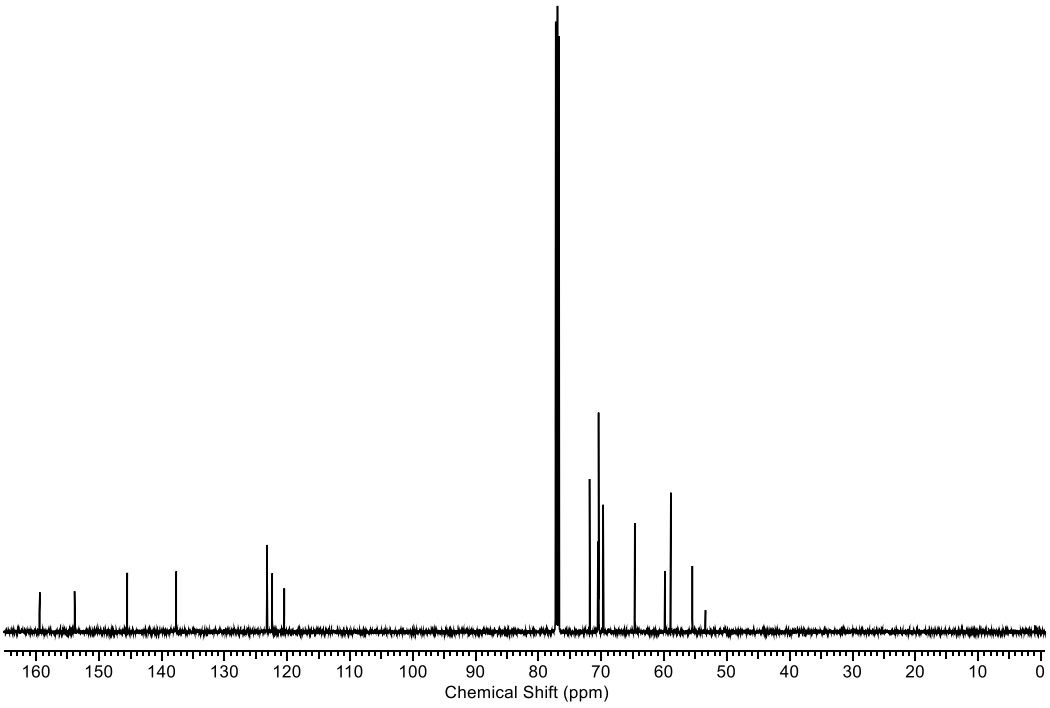

Figure S18. ^{13}C NMR of ligand **6H** in $CDCl_3$ (125 MHz, *T* = 298 K).

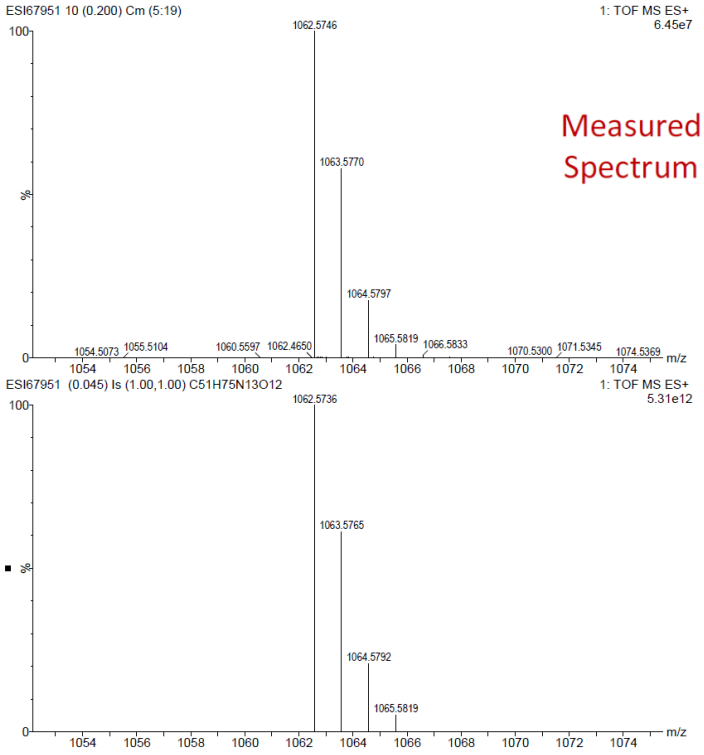

Figure S19. High-resolution mass spectrum of ligand **6H**.

Tripodal XB ligand, 6l

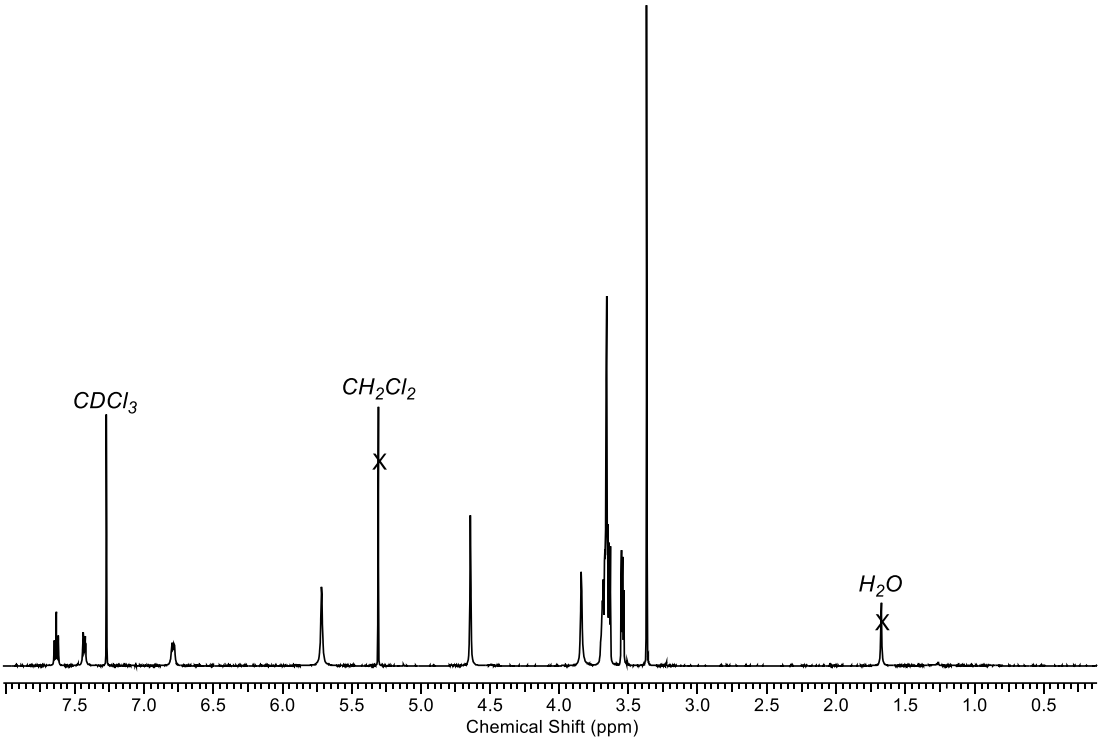

Figure S20. ^{1}H NMR of ligand **6l** in $CDCl_3$ (500 MHz, *T* = 298 K).

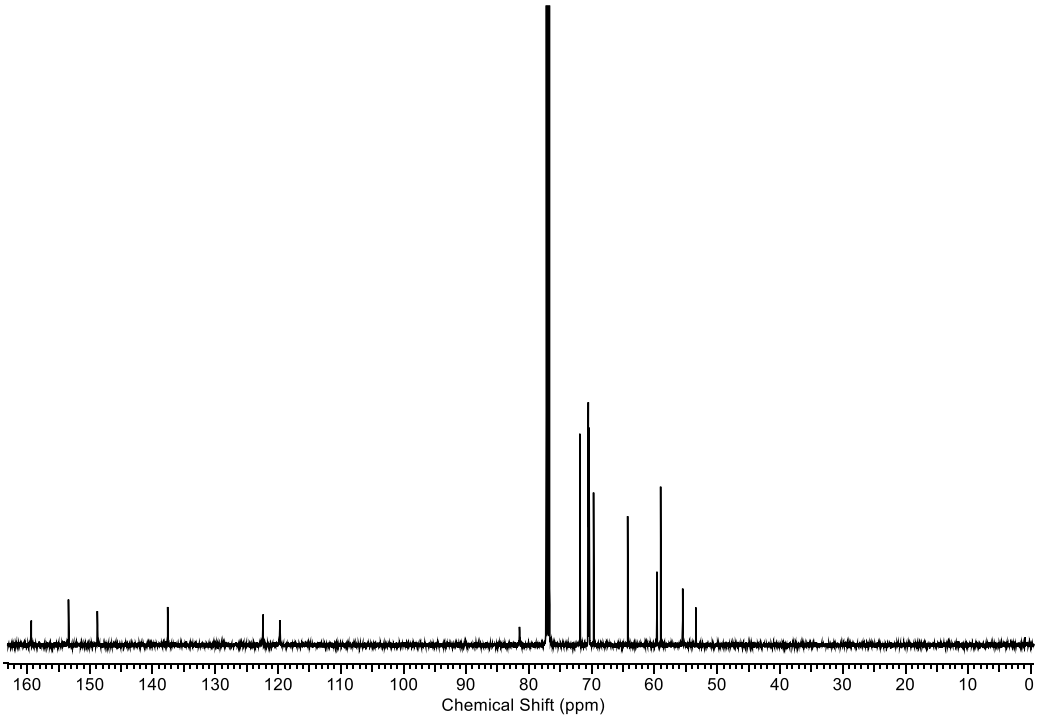

Figure S21. ^{13}C NMR of ligand **6l** in $CDCl_3$ (125 MHz, *T* = 298 K).

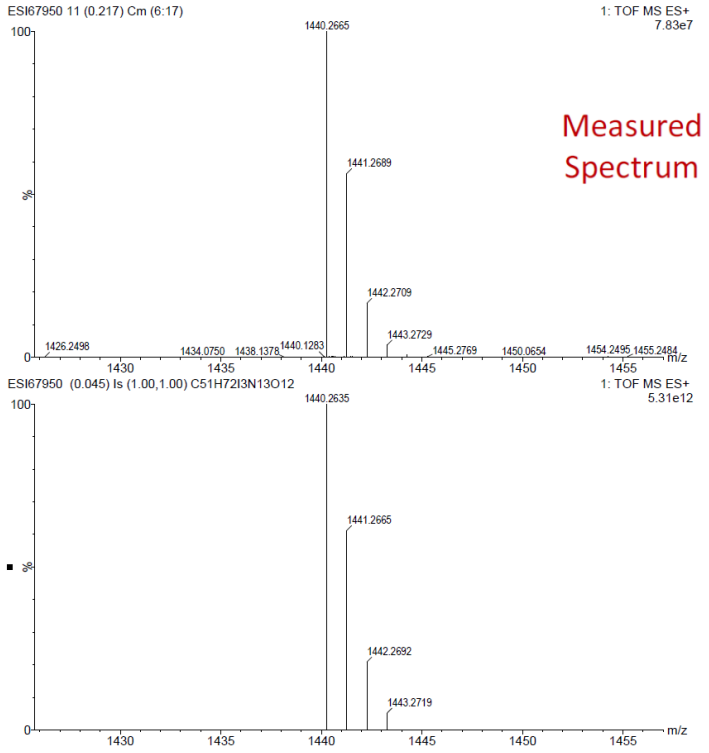

Figure S22. High-resolution mass spectrum of ligand **6l**.

Succinimidyl-3-propiolate, 7

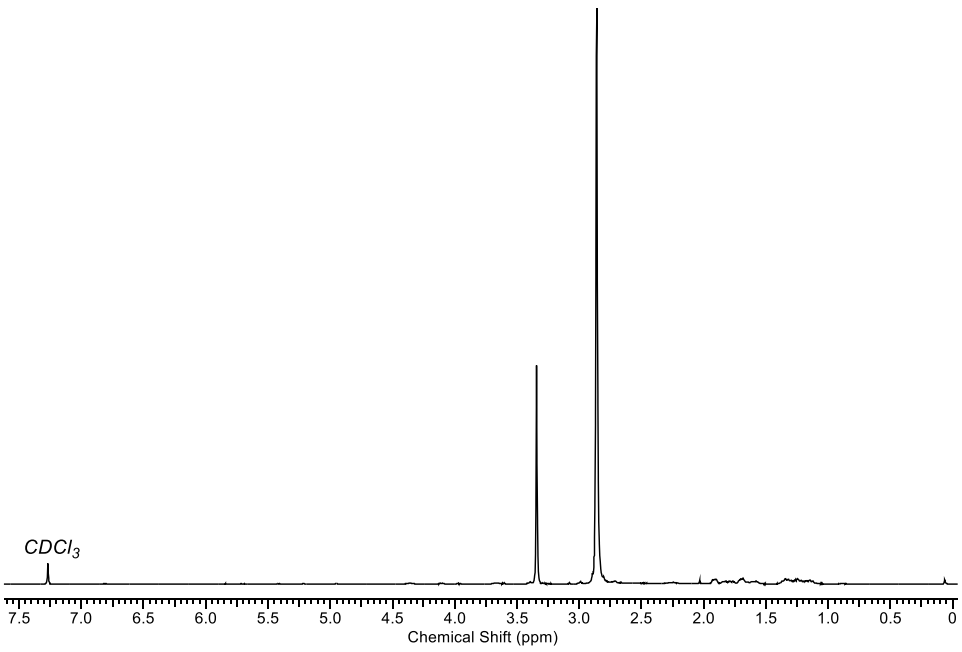

Figure S23. ^{1}H NMR of precursor **7** in $CDCl_3$ (500 MHz, *T* = 298 K).

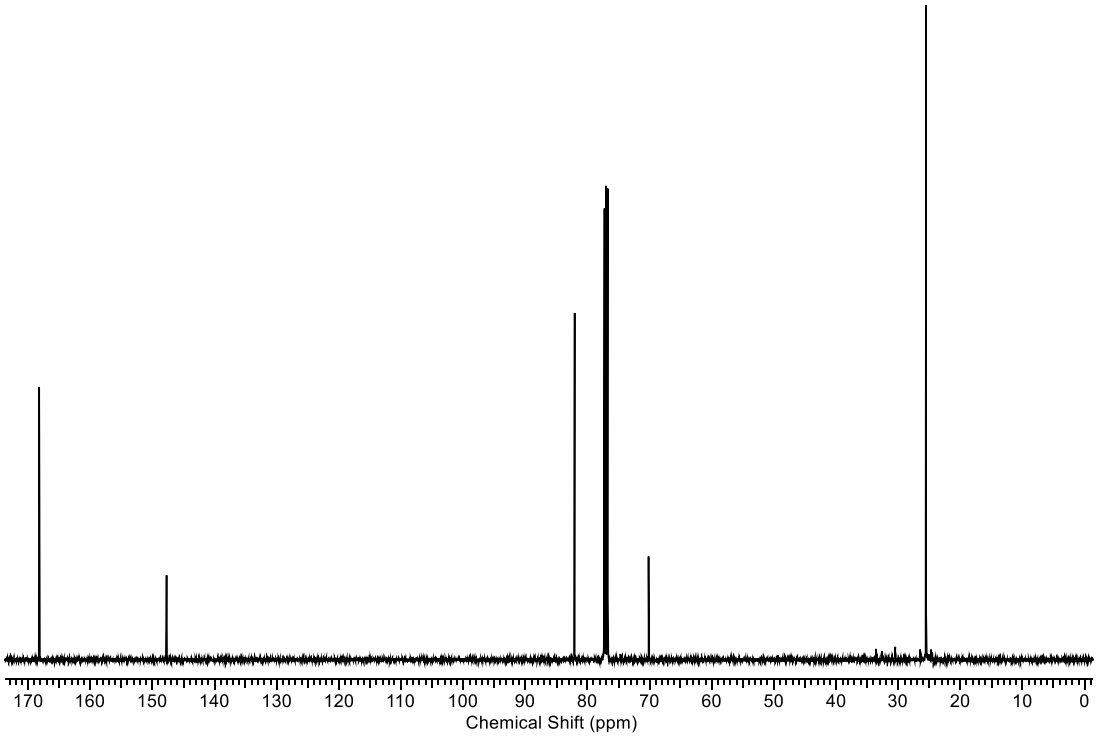

Figure S24. ^{13}C NMR of precursor **7** in $CDCl_3$ (125 MHz, *T* = 298 K).

6^{A}-amido-pmβCD alkyne, 9

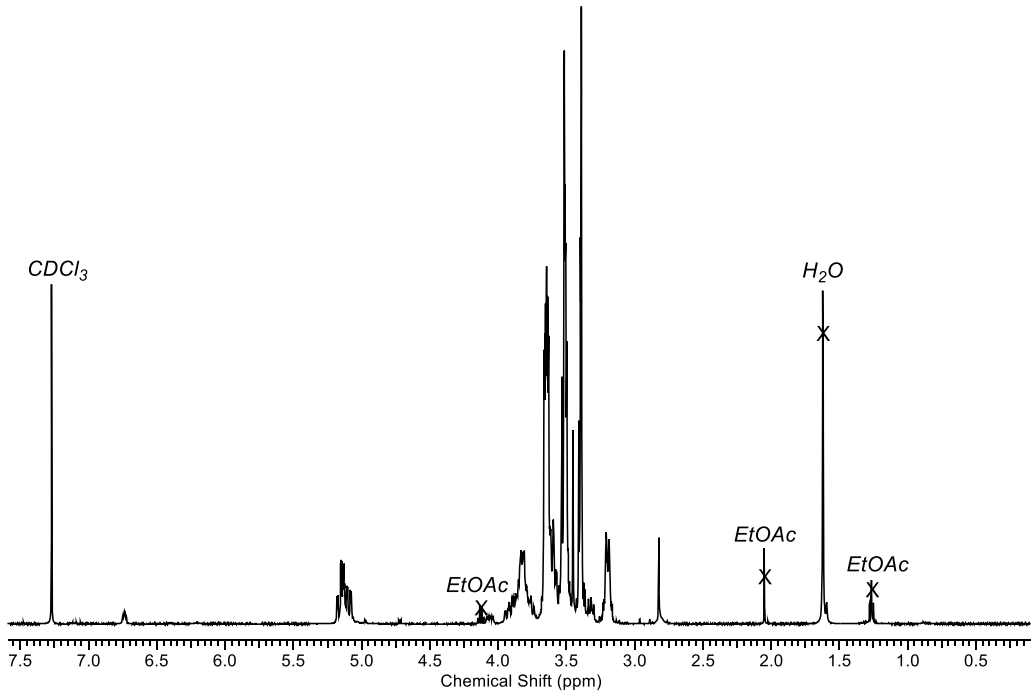

Figure S25. ^{1}H NMR of alkyne **9** in $CDCl_3$ (500 MHz, *T* = 298 K).

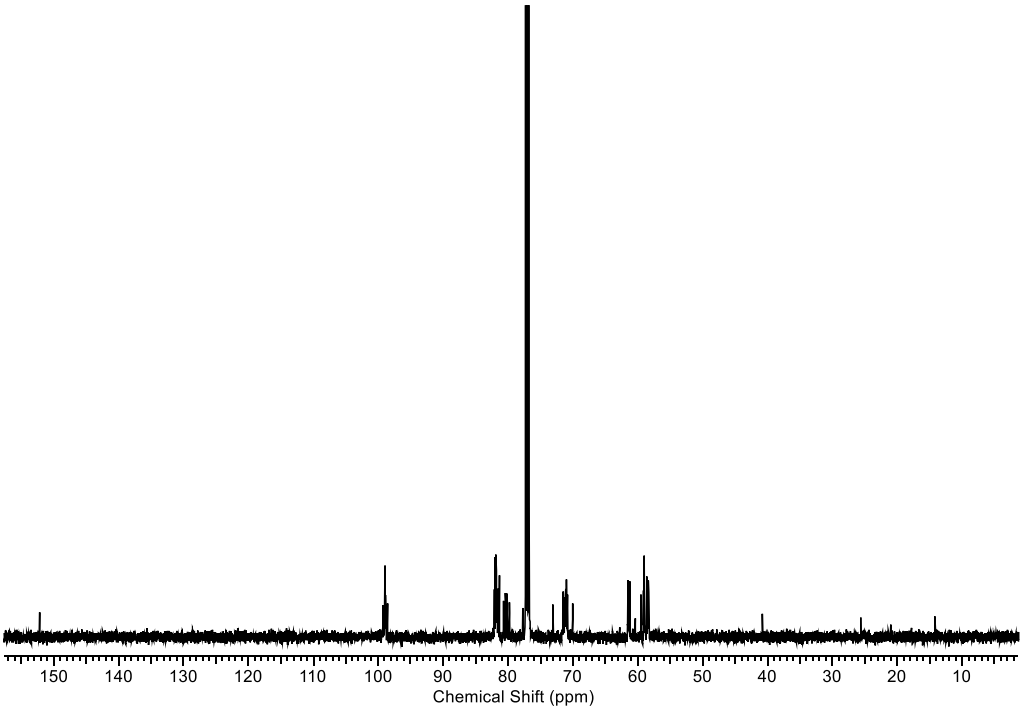

Figure S26. ^{13}C NMR of alkyne **9** in $CDCl_3$ (125 MHz, *T* = 298 K).

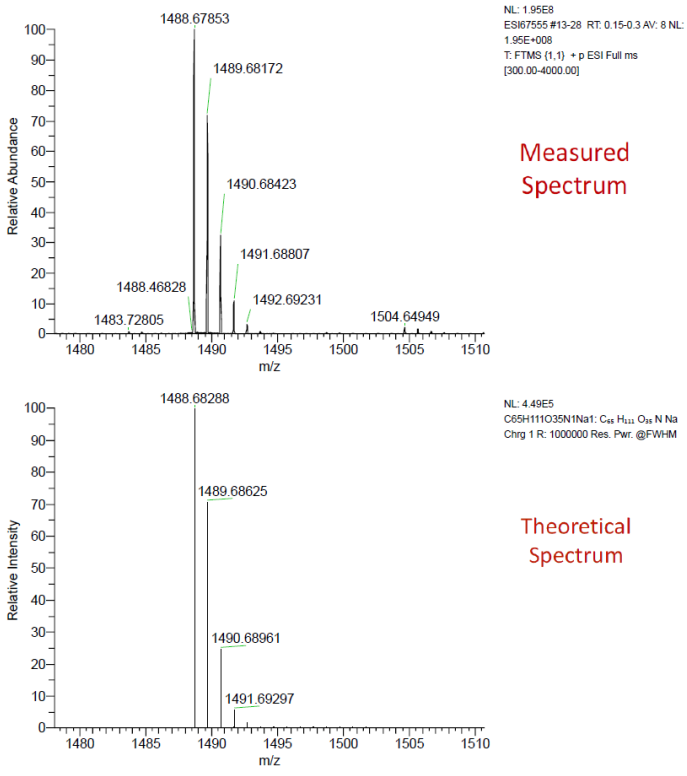

Figure S27. High-resolution mass spectrum of alkyne **9**.

6^A-amido-pmβCD-appended XB 'hydroxy-arm' precursor, 10l

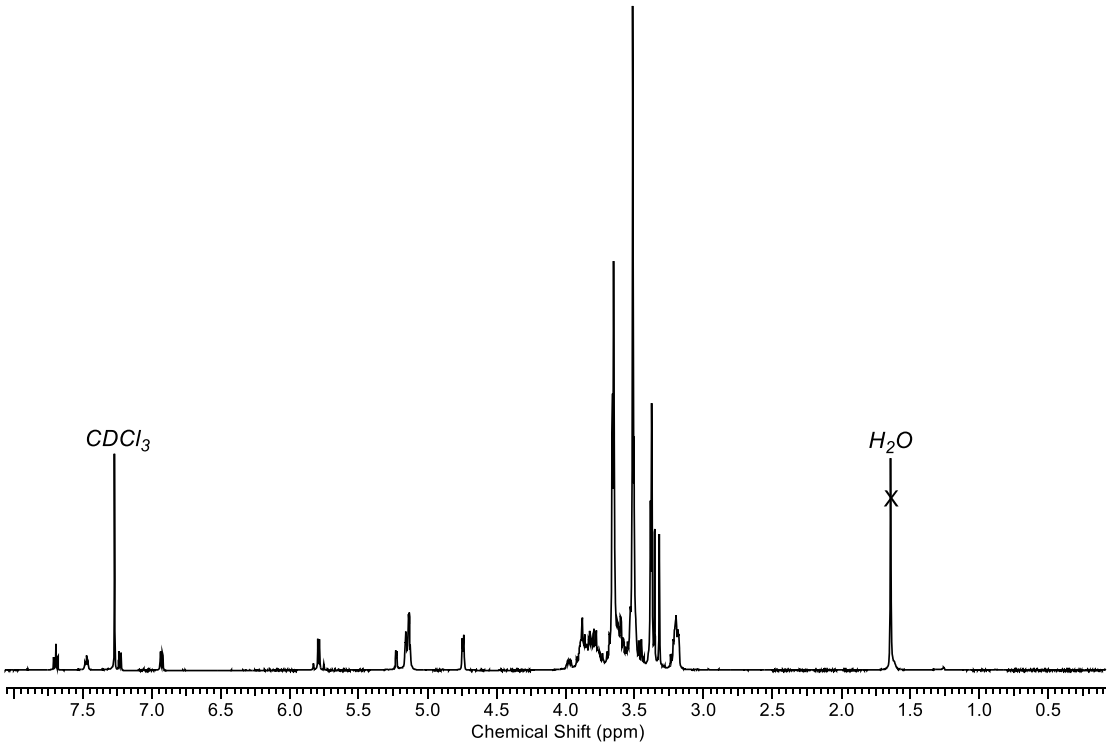

Figure S28. ^{1}H NMR of precursor **10l** in $CDCl_3$ (500 MHz, *T* = 298 K).

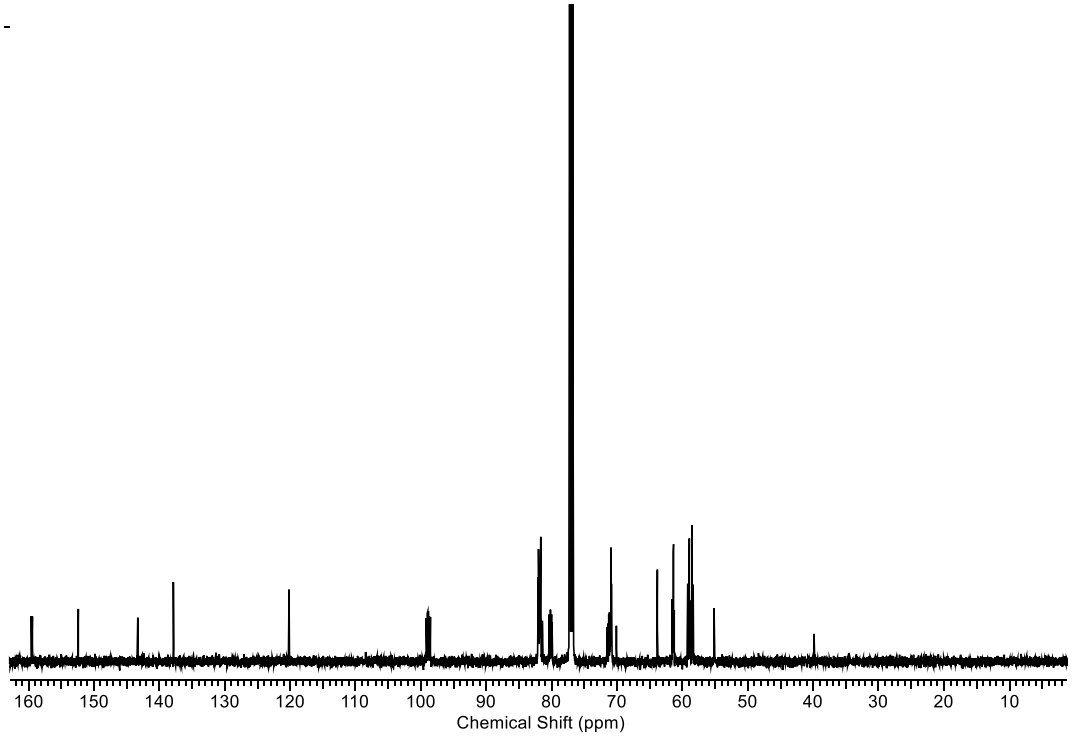

Figure S29. ^{13}C NMR of precursor **10l** in $CDCl_3$ (125 MHz, *T* = 298 K).

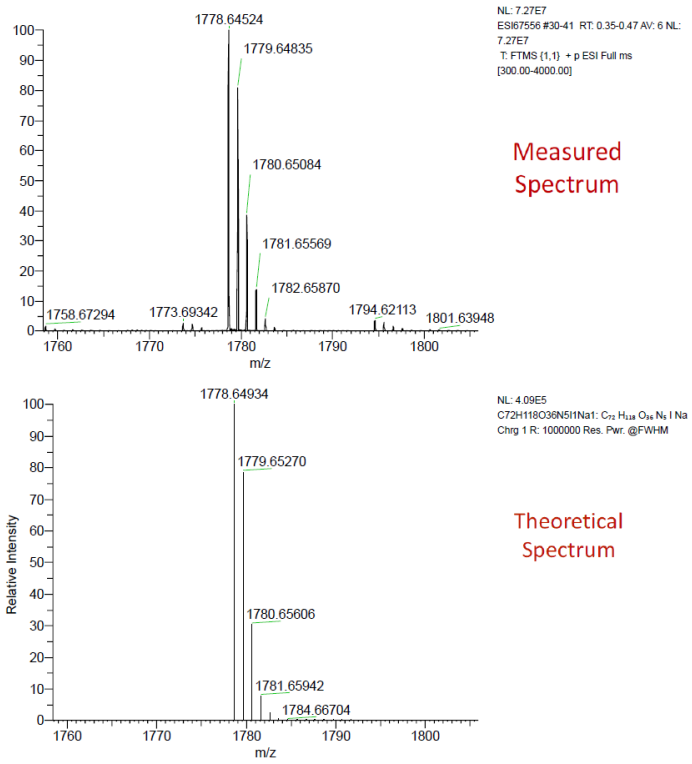

Figure S30. High-resolution mass spectrum of precursor **10I**.

6^{A}-amido-pmβCD-appended XB 'chloro-arm' precursor, 11I

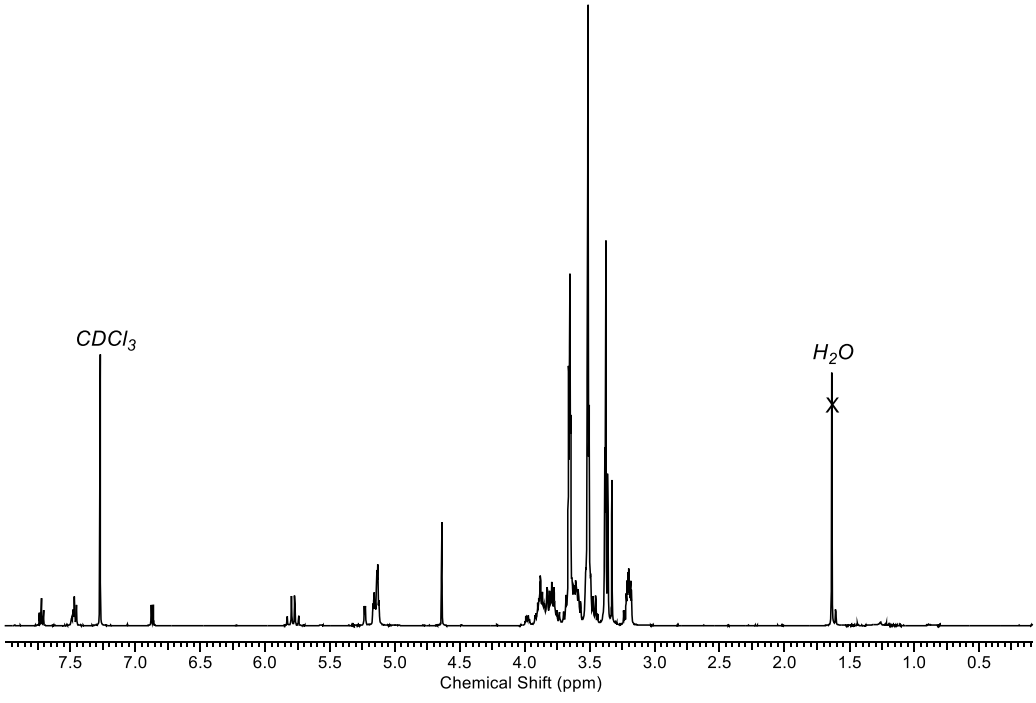

Figure S31. ^{1}H NMR of precursor **11I** in $CDCl_3$ (500 MHz, T = 298 K).

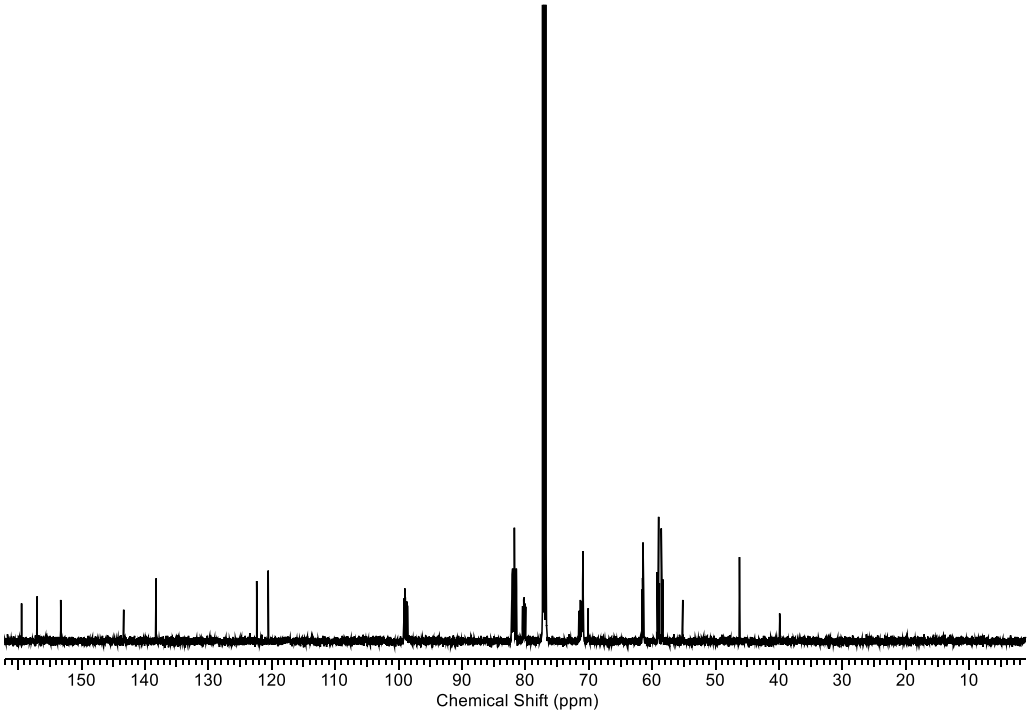

Figure S32. ^{13}C NMR of precursor **11l** in $CDCl_3$ (125 MHz, *T* = 298 K).

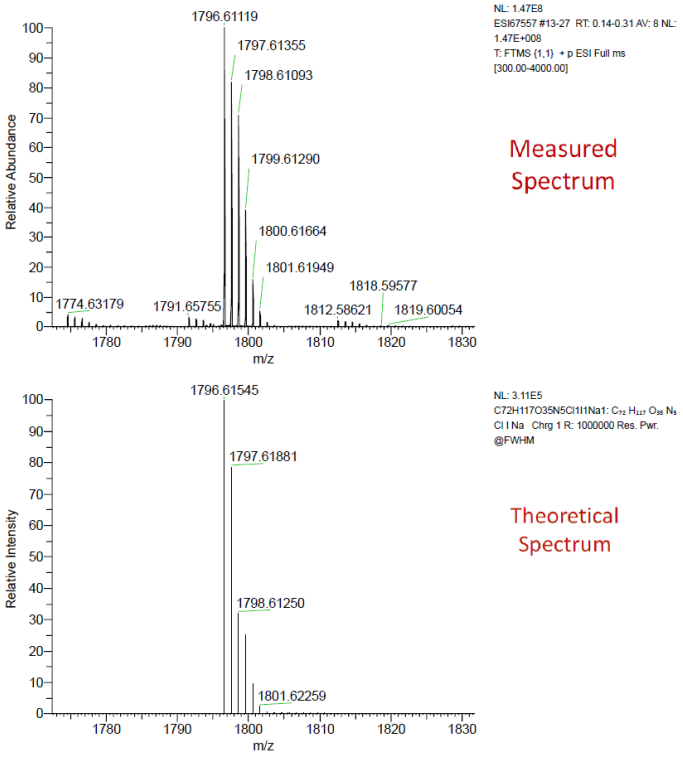

Figure S33. High-resolution mass spectrum of precursor **11l**.

Tris(pmβCD)-appended XB tripodal ligand, 12I

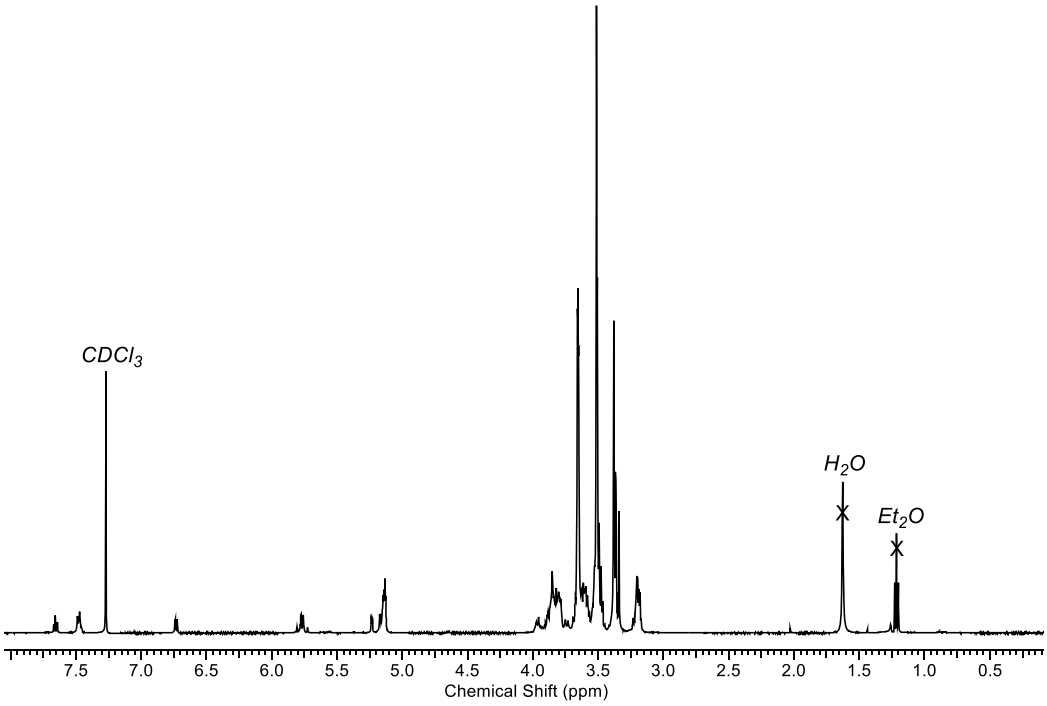

Figure S34. ^{1}H NMR of ligand **12I** in $CDCl_3$ (500 MHz, *T* = 298 K).

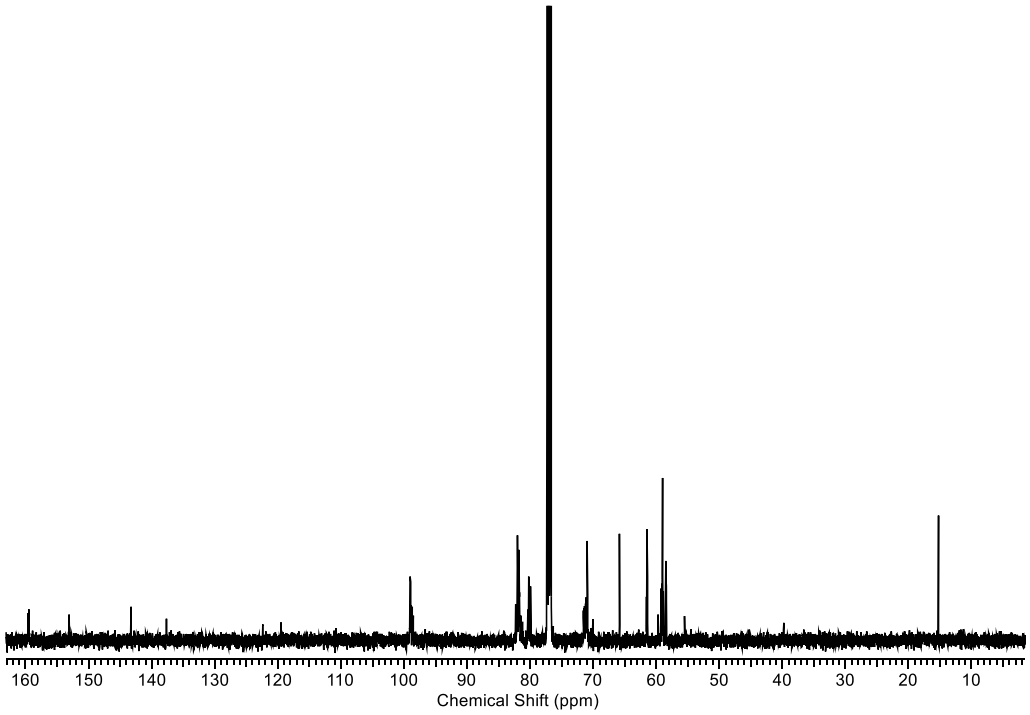

Figure S35. ^{13}C NMR of ligand **12I** in $CDCl_3$ (125 MHz, *T* = 298 K).

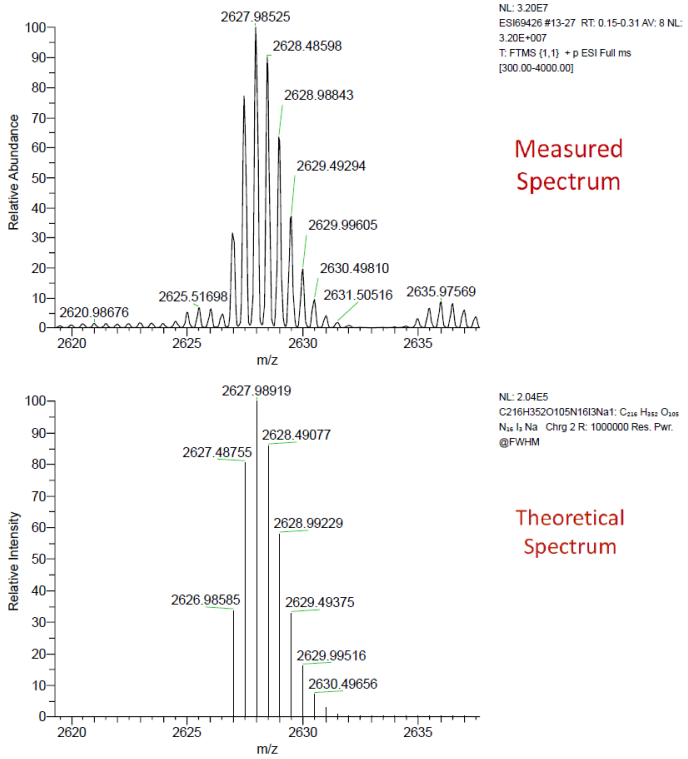

Figure S36. High-resolution mass spectrum of ligand **12I**.

S3.2 Further comparative ^{1}H NMR spectra of tripodal XB ligand formation

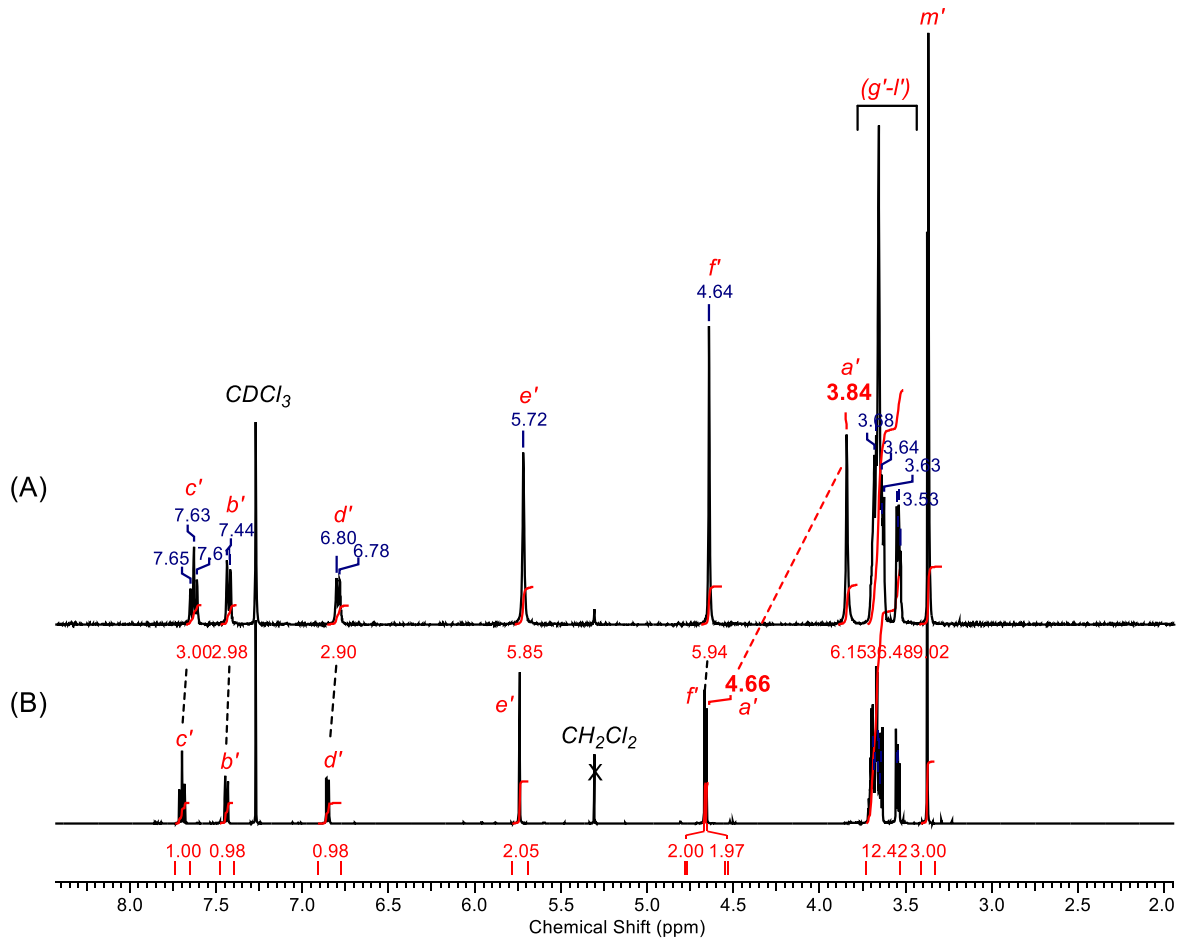

Figure S37. Stacked ^{1}H NMR spectra of (A) XB trimer **6l** and (B) synthon **5l** in $CDCl_3$ (500 MHz, *T* = 298 K). See Scheme 1 of the main paper for proton assignment.

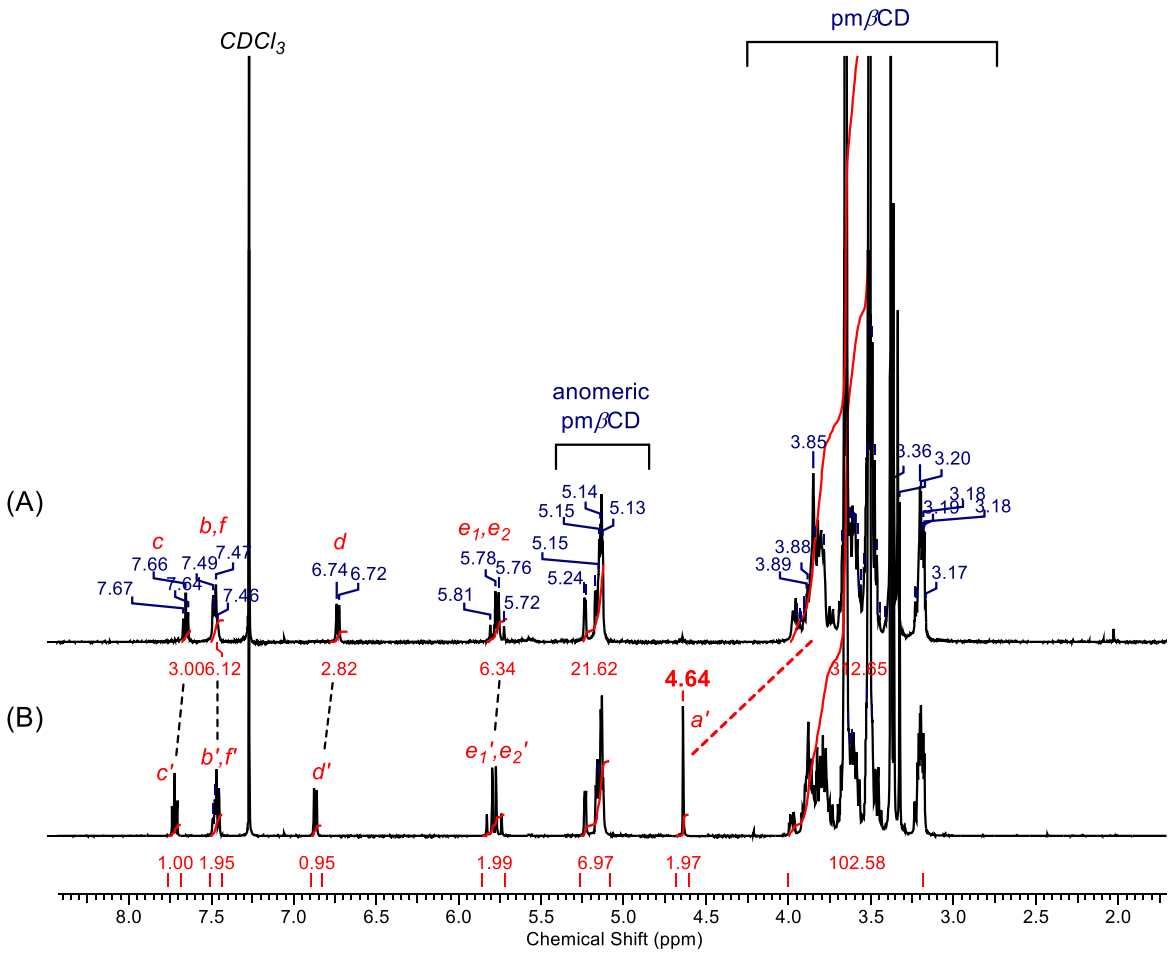

Figure S38. Stacked ^{1}H NMR spectra of (A) XB trimer **12I** and (B) synthon **11I** in $CDCl_3$ (500 MHz, *T* = 298 K). See Scheme 2 of the main paper for proton assignment. (The methylene H_e protons of both compounds are diastereotopic and hence appear as an AB quartet signal).

S3.3 UV-vis, EPR and HR-MS spectra of XB, HB Cu(II)-receptors

Tripodal XB Cu(II) receptor, 1I·2OTf

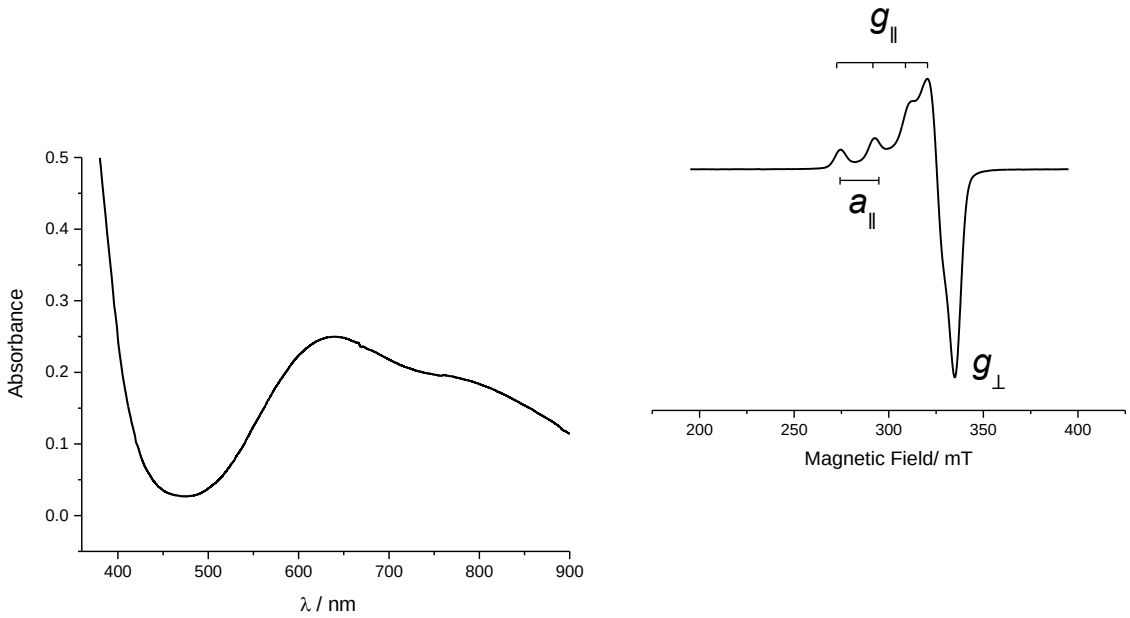

Figure S39. (left) UV-vis spectrum of **1I**·2OTf in CH_3CN/ H_2O 6:4 *v/v*, 10 mM HEPES ([host] = 2 mM, *T* = 293 K): peak absorption wavelengths $\lambda_{abs,max}$ (ε/ M^{-1} cm^{-1}) at 647 nm (117) and 775 nm (91) (shoulder); (right) the corresponding X-band EPR spectrum in frozen solution (*T* = 85 K): $g\parallel$ = 2.225 and $g\perp$ = 2.056 ($A\parallel$ = 183.0 x 10^{-4} cm^{-1}).

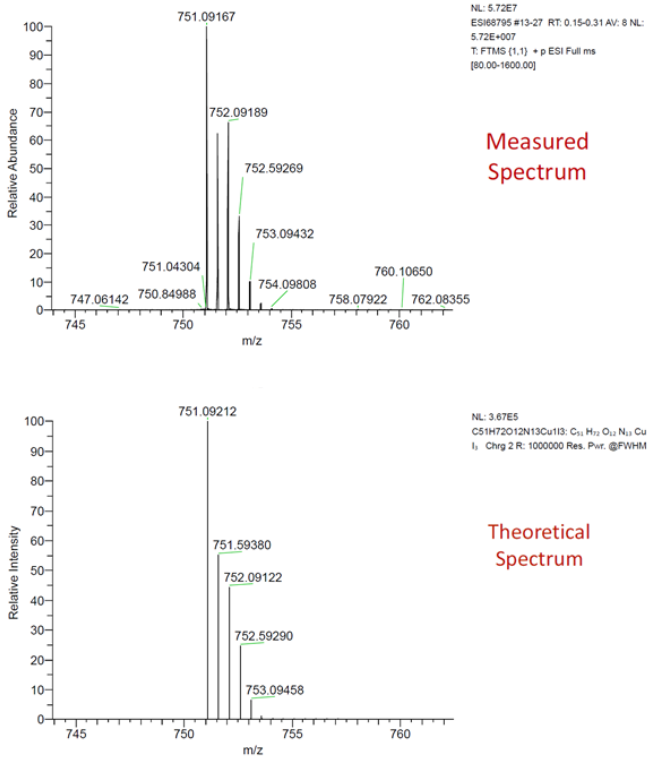

Figure S40. High-resolution mass spectrum of receptor **1I**·2OTf.

Tripodal HB Cu(II)-receptor, 1H·2OTf

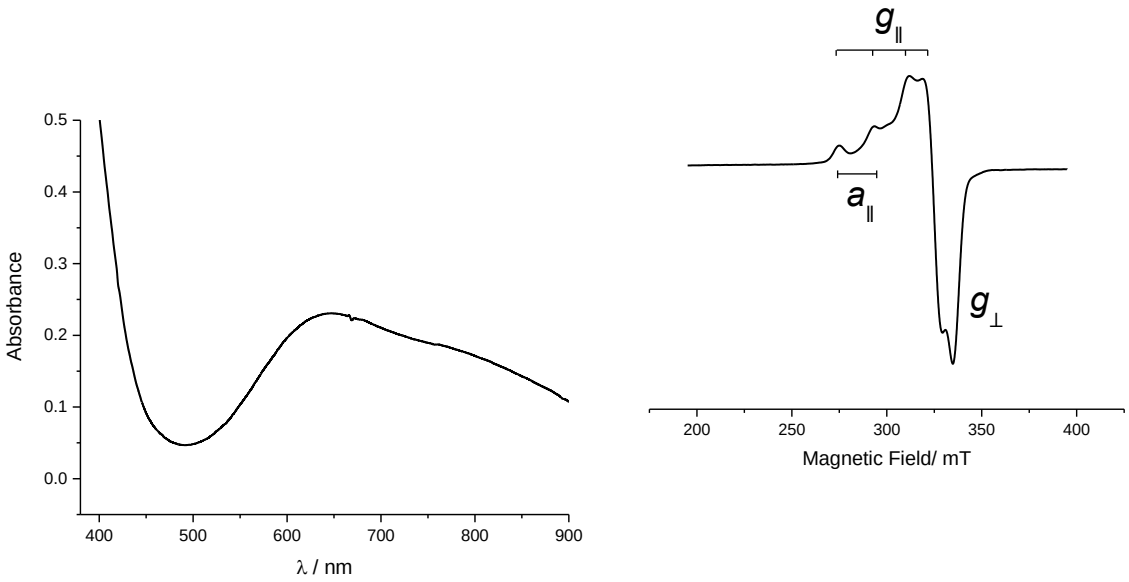

Figure S41. (left) UV-vis spectrum of **1H**·2OTf in CH_3CN/ H_2O 6:4 *v/v*, 10 mM HEPES ([host] = 2 mM, *T* = 293 K): peak absorption wavelengths $\lambda_{abs,max}$ (ε/ M^{-1} cm^{-1}) at 639 nm (125) and 760 nm (98) (shoulder); (right) the corresponding X-band EPR spectrum in frozen solution (*T* = 85 K): $g\parallel$ = 2.285 and $g\perp$ = 2.055 ($A\parallel$ = 180.0 x 10^{-4} cm^{-1}).

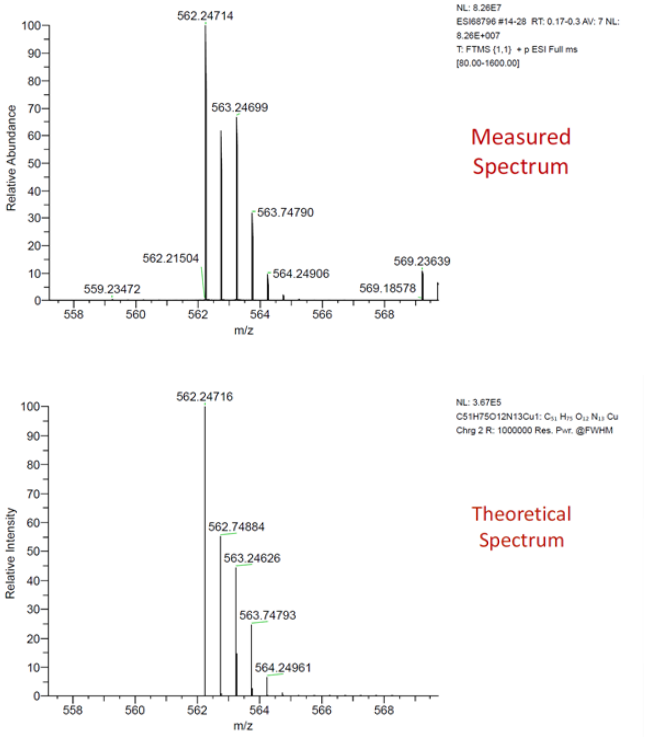

Figure S42. High-resolution mass spectrum of receptor **1H**·2OTf.

Tripodal XB Cu(II) receptor, 13I·2OTf

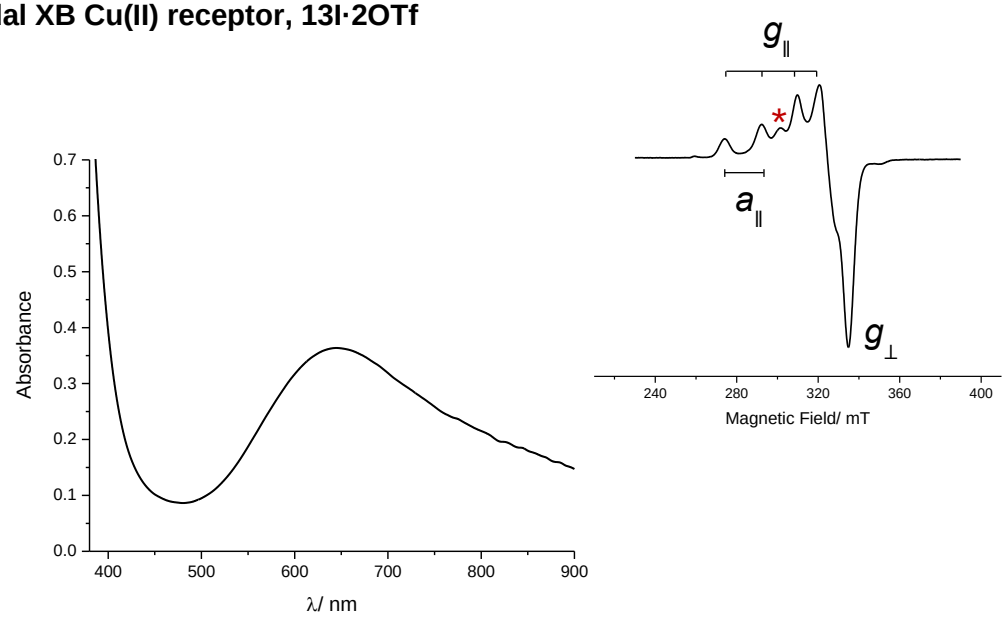

Figure S43. (left) UV-vis spectrum of **13I**·2OTf in CH_3CN/ H_2O 6:4 *v/v*, 10 mM HEPES (2 mM, *T* = 293 K): peak absorption wavelengths $\lambda_{abs,max}$ (ε/ M^{-1} cm^{-1}) at 645 nm (182) and 770 nm (119) (shoulder); (right) the corresponding X-band EPR spectrum in frozen solution (*T* = 85 K): $g\parallel$ = 2.225 and $g\perp$ = 2.065 ($A\parallel_1$ = 185.0 x 10^{-4} cm^{-1}, $A\parallel_2$ = 220.0 x 10^{-4} cm^{-1}).

N.B. the asterisk denotes a smaller, secondary component of the EPR spectral signature, which is suggestive of a minority receptor species where there is a subtle difference in the coordination geometry of the Cu(II) center compared to that discussed in the main paper – possibly, a consequence of the nature of the sterically bulky pmβCD-appendages which affect the metal's coordination sphere in frozen solution.

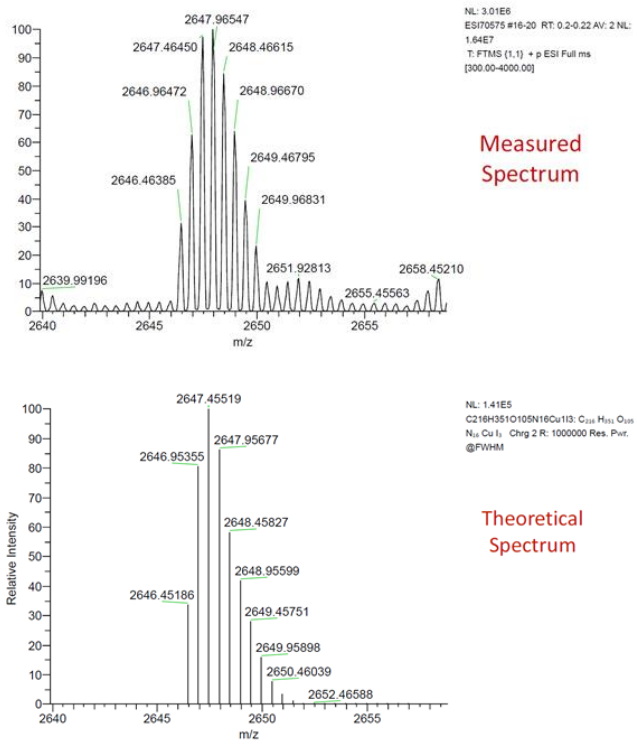

Figure S44. High-resolution mass spectrum of receptor **13I**·2OTf.

S4. Isothermal Titration Calorimetry (ITC) Studies and Data

S4.1 General comments and titration protocols

All isothermal titration calorimetry experiments were performed on a Microcal PEAQ-ITC automated system, utilising unbuffered distilled water at T = 298 K.

M^{2+} titration protocol for **6I** and **13I**

An initial concentration of the XB tripodal ligand of 0.5 mM was used, with a 4 mM solution of $CuOTf_2$ added in 35 aliquots. The data from the first addition of 0.5 µL was discarded, with data collected for the subsequent 34 additions of 1 µL. Heats of dilution were measured by a preliminary titration of individual solutions of the respective metal salt into unbuffered water. Values of K_a and ΔH were calculated using the MicroCal PEAQ-ITC Analysis Software, *via* a non-linear least squares regression fit of the experimental data to the one-set-of-sites model. These values were then used to determine the ΔG and ΔS values.

S4.2 ITC Data

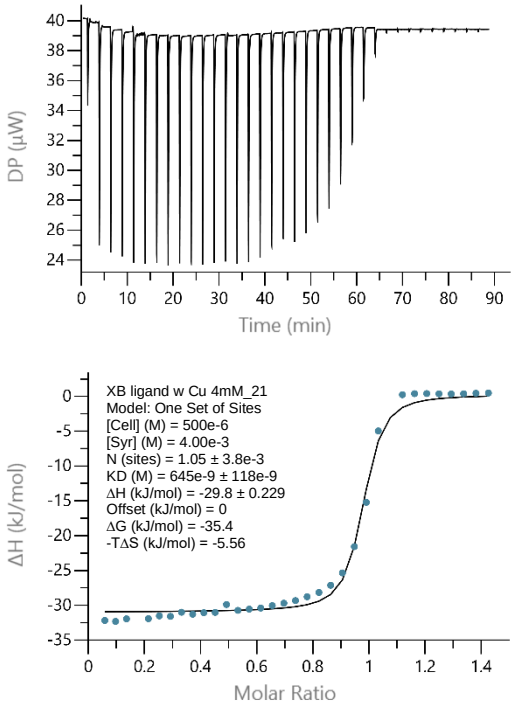

Figure S45. (top) Raw ITC data for the sequential addition of $CuOTf_2$ to **6l** (unbuffered water, *T* = 298 K); (bottom) integrated heat plot obtained from titration.

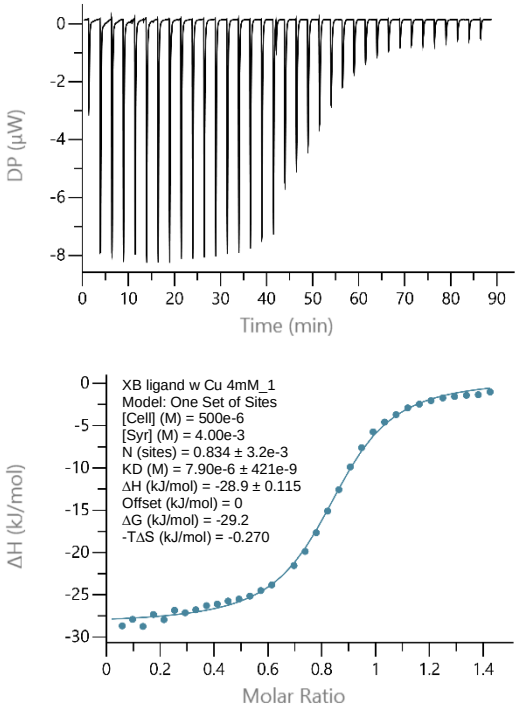

Figure S46. (top) Raw ITC data for the sequential addition of $CuOTf_2$ to **12I** (unbuffered water, *T* = 298 K); (bottom) integrated heat plot obtained from titration.

S5. UV-vis Experiments

S5.1 General information and titration protocol

All UV-vis spectroscopy titrations were performed on a T60U (PG Instruments Ltd) spectrophotometer and the data processed using the OriginPro 2015 software package. In each case, titrations were performed in the stated solvent systems at *T* = 293 K, using a standard 1 mL Hellma quartz cuvette with path length of 1 cm

M^{2+} titration protocol for **6I** with Cu(II) in CH_3CN

A 0.75 mL initial volume of the host was used at a concentration of 2 mM. A 15 mM solution of the cationic Cu(II) guest was prepared by dissolving copper triflate salt in a solution containing the same concentration of the host (*i.e.* 2 mM). Aliquots of the Cu(II) solution were added to the UV-vis cuvette, the samples thoroughly mixed using a syringe needle and the absorption spectra recorded at 0, 0.1, 0.2, 0.3, 0.4, 0.5, 0.6, 0.7, 0.8, 0.9, 1.0, 1.2, 1.4, 1.6, 1.8 and 2.0 equivalents of cation (0.1 eq = 10 µL). The absorbances for each addition, at a chosen wavelength (640 nm), were used to calculate the delta absorbances relative to the first absorbance reading. These values were then plotted versus the equivalents of the added Cu(II) guest for each aliquot, to obtain a qualitative isotherm which affirmed the expected 1:1 stoichiometry of ligand to metal binding.

Anion titration protocol for **1I**·2OTf, **1H**·2OTf and **13I**·2OTf in CH_3CN/ H_2O 6:4 *v/v* (at pH 6.3 with 10 mM HEPES)

In a typical titration experiment, a 0.75 mL initial volume of the host was used at a concentration of 2 mM, with 600 mM solutions of anion guests. Specifically, each of the anion solutions were prepared by dissolving the tetrabutylammonium salt of the desired anion in a solution containing the same concentration of the host (*i.e.* 2 mM), to ensure that the total host concentration remained constant throughout the titration - thus any absorption changes could be reasonably attributed to anion complexation and not dilution effects upon anion addition. Aliquots of anion solutions (1.0 eq = 2.5 µL) were added to the UV-vis cuvette, the samples thoroughly mixed using a syringe needle and the changes in the absorption spectra recorded from 0 equivalents to up to 100 equivalents of anion, with at least 15 data sets collected, until saturation of the binding curve was seen. After each aliquot addition, the spectra were recorded at least twice till consistent spectra were obtained. Association constants were calculated from the UV-vis titration data by non-linear global fitting analysis to a host-guest 1:1 or 1:2 stoichiometric binding model (as appropriate) using the Bindfit[7] software, monitoring the change in absorbance in the range 800–850 nm.

N.B. The interaction of Cu(II) with the zwitterionic HEPES buffer has previously been shown to be negligible[8] and hence the observed changes in the UV-vis titration spectra were attributed to arise invariably from the interactions of the guest anions with the respective Cu(II)-host.

S5.2 UV-vis titration data and isotherms

(A) XB Cu(II)-Tripod **1I**·2OTf

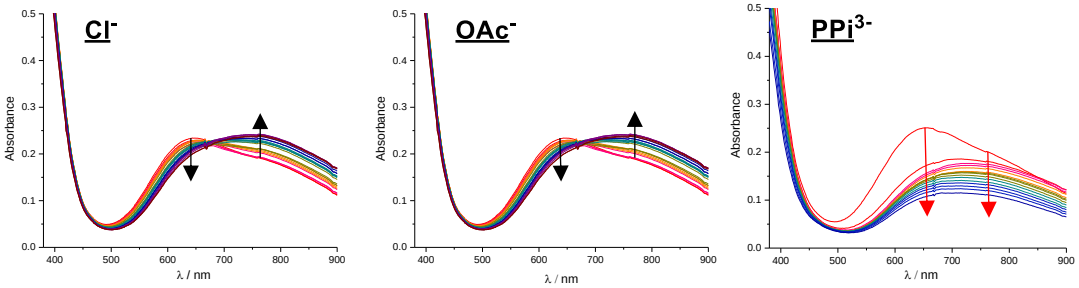

(B) HB Cu(II)-Tripod **1H**·2OTf

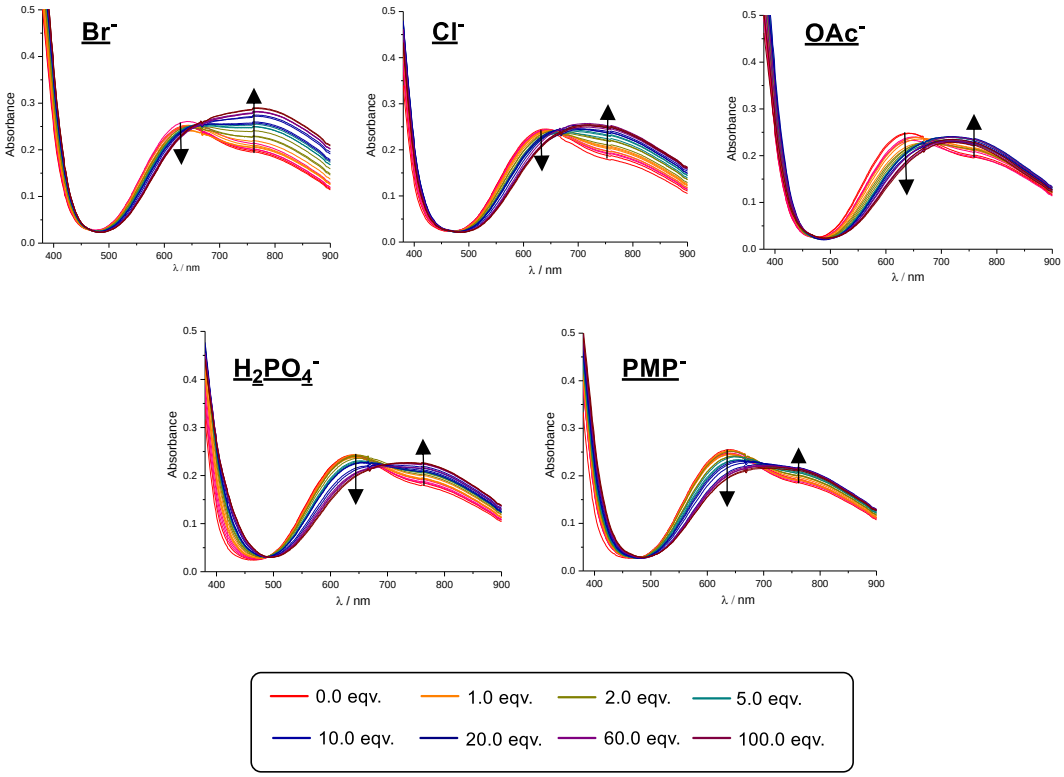

Figure S47. UV-vis titration spectra of (A) **1I**·2OTf and (B) **1H**·2OTf in the presence of up to 120 equivalents of various anions ([host] = 2 mM, CH_3CN/H_2O 6:4 buffered with 10 mM HEPES at pH 6.3, *T* = 293 K).

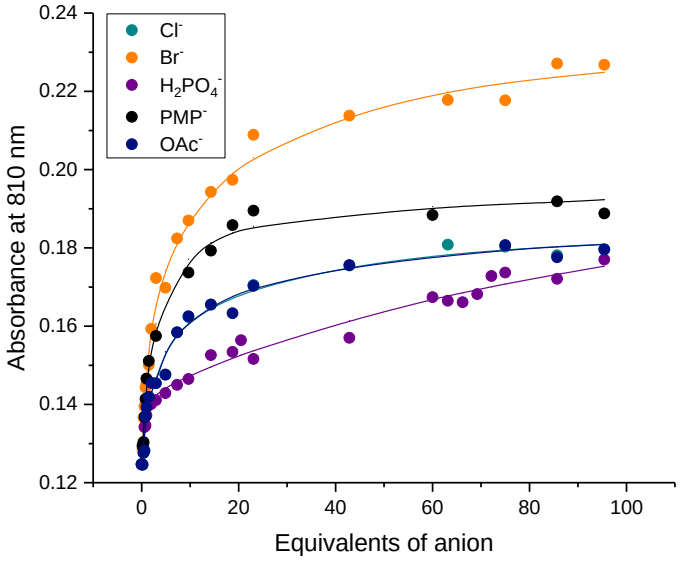

Figure S48. Plots of change in absorbance of **1I**·2OTf at 810 nm against equivalents of anion added ([host] = 2 mM, CH_3CN/H_2O 6:4 buffered with 10 mM HEPES at pH 6.3, *T* = 293 K).

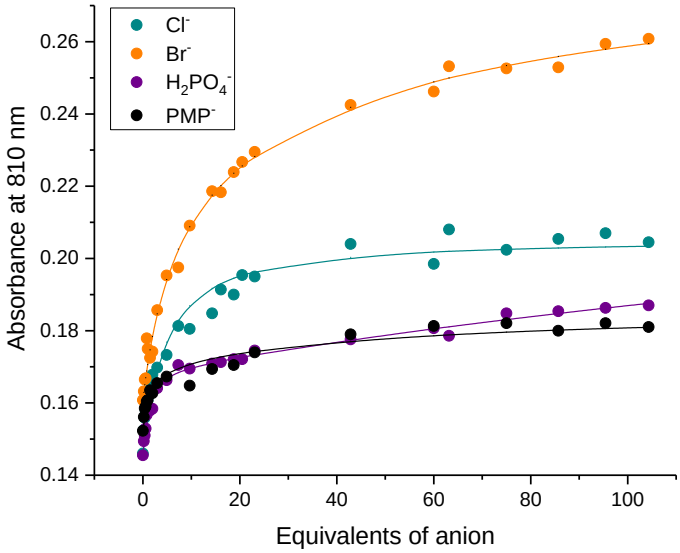

Figure S49. Plots of change in absorbance of **1H**·2OTf at 810 nm against equivalents of anion added ([host] = 2 mM, CH_3CN/H_2O 6:4 buffered with 10 mM HEPES at pH 6.3, *T* = 293 K).

S6. EPR Experiments

S6.1 General information and titration protocol

All EPR spectroscopy titrations were performed on a Bruker EMXmicro continuous wave (CW) spectrometer (X-band) and the data processed using the OriginPro 2015 software package. In each case, titrations were performed in the stated solvent system at T = 293 K and the EPR spectra recorded at T = 85 K.

Anion titration protocol for **1I**·2OTf and **1H**·2OTf in CH_3CN/ H_2O 6:4 *v/v* (at pH 6.3 with 10 mM HEPES)

In a typical titration experiment, a 0.75 mL initial volume of the host was used at a concentration of 2 mM, with 600 mM solutions of anion guests. Specifically, each of the anion solutions were prepared by dissolving the tetrabutylammonium salt of the desired anion in a solution containing the same concentration of the host (*i.e.* 2 mM), to ensure that the total host concentration remained constant throughout the titration - thus any spectral intensity changes could be reasonably attributed to anion complexation and not dilution effects upon anion addition. Aliquots of anion solutions (1.0 eq = 2.5 µL) were added to a solution of the host in a cuvette, the sample thoroughly mixed using a syringe needle and 100 µL of this host-guest solution taken for the EPR measurement. The sample solution in the EPR tube was then recombined with the rest of the solution in the cuvette, and the procedure repeated with the next addition of anion equivalents (up to 100 equivalents). At least 15 data sets of the changes in the EPR spectra were recorded, until saturation of the binding curve was seen. Anion association constants were calculated from the EPR titration data by non-linear global fitting analysis to a host-guest 1:2 stoichiometric binding model using the Bindfit[7] software, monitoring the change in spectral signature intensity in the range 280-290 mT for both XB/HB receptors.

S7. Electrochemical Anion Sensing Studies

S7.1 General comments and titration protocols

All Cyclic voltammetry (CV), differential pulse voltammetry (DPV) and square wave voltammetry (SWV) voltammetric measurements were performed using an Autolab Potentiostat/Galvanostat model PG-STAT 12 (Metrohm Autolab, Netherlands), using a standard single compartment three-electrode electrochemical cell placed inside a Faraday cage and the data processed using the OriginPro 2015 software package. In each case, titrations were performed in the stated solvent systems at T = 293 K.

Titration protocol for **1I**·2OTf and **1H**·2OTf in CH_3CN

The same three-electrode cell was used with the same working and counter electrodes as stated above except using a Ag/ AgCl (3.4 M KCl) leak-free reference electrode (Innovative Instruments) in a 0.1 M $TBAClO_4$ supporting electrolyte solution. All experiments were conducted in Argon purged solutions under an Argon blanket. The working electrode was polished with alumina slurry (0.05 µm) before each experiment. (In order to circumvent the development of junction potentials of the latter reference electrode in the presence of various ions a Ag/ AgCl reference electrode with a Pt wire frit was utilized for titration experiments). Prior to performing redox titration experiments, the redox reversibility of each receptor was first studied by recording successive CV scans at scan rates of 25, 50, 75, 100, 200, 400, 600 and 800 mV s^{-1}. After establishing receptor redox quasi-reversibility and reproducibility of each receptor's Cu^{I}/Cu^{II} $E_{1/2}$ value, electrochemical SWV titrations were carried out using a 0.9 mL initial volume of the host at a concentration of 0.5 mM and the measurements recorded with 1 s equilibration time, utilising a frequency of 25 Hz, an amplitude of 20 mV and a step potential of 2 mV. A 100 mM solution of TBA Br was added in aliquots, the samples thoroughly mixed by mechanical agitation and the voltammograms recorded at 0, 1.0, 2.0, 10.0, 20.0, 35.0, 60.0 and 100.0 equivalents of anion (1.0 eq = 4.5 µL). The delta $E_{1/2}$ values were recorded and plotted against the concentration of anion. The resulting binding isotherms were curve fit as described by Schöllhorn.[9]

Electrochemical reversibility studies of **1I**·2OTf and **1H**·2OTf in water were also performed by recording CV scans (at the same scan rates as above) and a SWV voltammogram (using the same parameters as above). The same three-electrode cell was used as above, with the same working, counter and reference electrodes instead in a 0.05 M KPF_6 supporting electrolyte solution. A host solution of 0.25 mM was used for all measurements.

S7.2 Criteria for reversibility

For a reversible electrochemical system displaying fast electron transfer kinetics, the following criteria needs to be met:

- E_{pa} and E_{pc} independent of scan rate
- $I_{pa}/ I_{pc} = 1$
- $\Delta E_p = (E_{pa} – E_{pc}) = (59/n)$ mV, where n is the number of electrons transferred during the redox process. Therefore, for a one-electron transfer process, the difference = 59 mV.
- I_{pa} and I_{pc} varies proportionally to the square root of the scan rate.

For all of the following receptors described herein, E_{pa} and E_{pc} were almost independent of scan rate at lower rates. With a few exceptions, I_{pa} / I_{pc} are typically in the range of 0.90 – 1.10 and ΔE_p show notable variations from 60 mV to 260 mV. In all cases, I_{pa} and I_{pc} vary almost proportionally with the square root of the scan rate (Pearsons's $R^2 > 0.94$). Thus the redox-active hosts generally showed 'quasi-reversible' electrochemical behaviour.

S7.3 Electrochemical Reversibility Studies

XB Cu(II)-tripod, 1I·2OTf

Studies performed in 0.1 M $TBAClO_4$ in anhydrous CH_3CN.

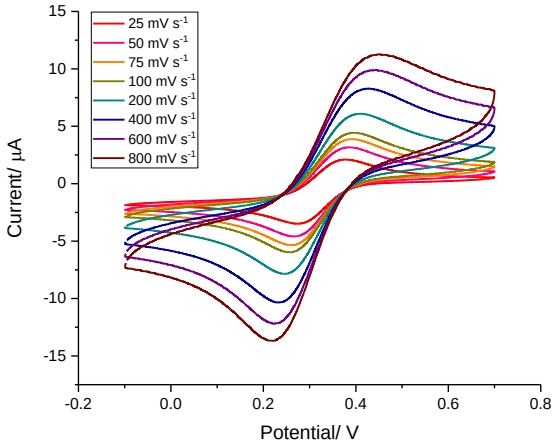

Figure S50. CV's of **1I**·2OTf at different scan rates ([host] = 0.5 mM, *T* = 293 K).

Table S1. Values of E_{pc}, E_{pa}, I_{pc}, I_{pa}, ΔE and I_{pa}/I_{pc} for **1I**·2OTf at different scan rates.

Scan rate/ mV s^{-1}	E_{pa}/ V	E_{pc}/ V	I_{pa}/ µA	I_{pc}/ µA	ΔE_p/ V	I_{pa}/I_{pc}
25	0.381	0.268	3.119	3.284	0.113	0.949
50	0.391	0.266	4.143	4.372	0.125	0.948
75	0.393	0.261	4.764	5.173	0.132	0.921
100	0.395	0.256	5.219	5.683	0.139	0.918
200	0.403	0.246	6.839	7.441	0.157	0.919
400	0.422	0.232	8.808	9.957	0.19	0.885
600	0.439	0.222	9.947	11.297	0.217	0.880
800	0.481	0.219	10.084	12.149	0.262	0.830

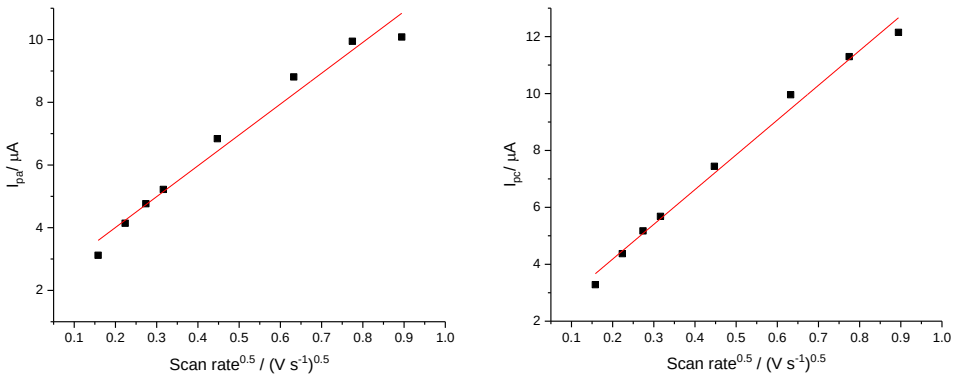

Figure S51. Plots of (left) I_{pa} and (right) I_{pc} against (scan rate)$^{1/2}$ for **1I**·2OTf.

HB Cu(II)-tripod, 1H·2OTf

Studies performed in 0.1 M $TBAClO_4$ in anhydrous CH_3CN.

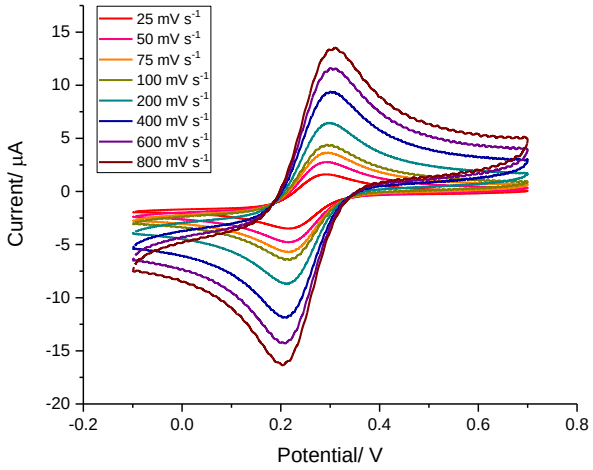

Figure S52. CV's of **1H**·2OTf at different scan rates ([host] = 0.5 mM, *T* = 293 K).

Table S2. Values of E_{pc}, E_{pa}, I_{pc}, I_{pa}, ΔE and I_{pa}/I_{pc} for **1H**·2OTf at different scan rates.

Scan rate/ mV s^{-1}	E_{pa}/ V	E_{pc}/ V	I_{pa}/ µA	I_{pc}/ µA	ΔE_p/ V	I_{pa}/I_{pc}
25	0.288	0.219	2.951	2.883	0.069	1.024
50	0.290	0.215	4.191	4.192	0.075	0.999
75	0.295	0.210	5.051	5.074	0.085	0.995
100	0.293	0.210	5.744	5.839	0.083	0.984
200	0.295	0.210	8.029	8.384	0.085	0.958
400	0.300	0.205	10.981	11.442	0.095	0.959
600	0.302	0.205	13.161	13.821	0.097	0.952
800	0.310	0.202	14.892	15.642	0.108	0.952

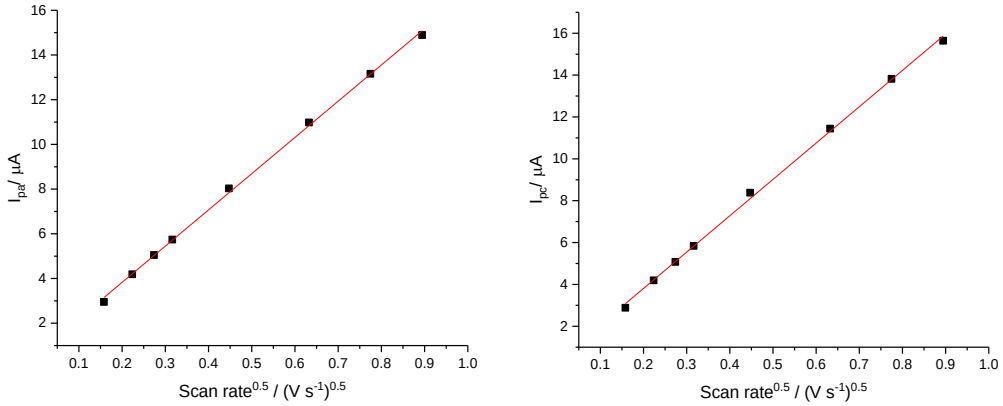

Figure S53. Plots of (left) I_{pa} and (right) I_{pc} against (scan rate)$^{1/2}$ for **1H**·2OTf.

XB Cu(II)-tripod, 1I·2OTf

Studies performed in 0.05 M KPF_6 in pure H_2O.

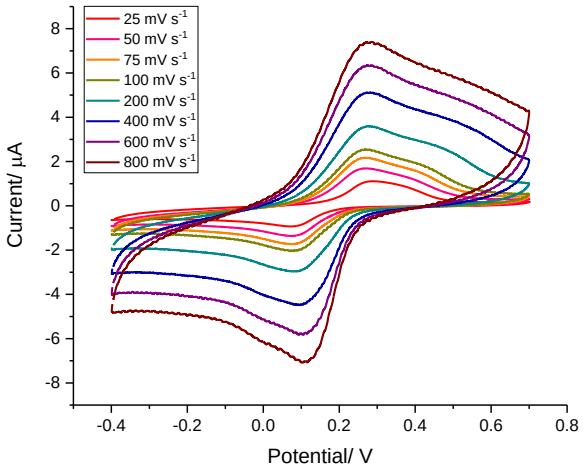

Figure S54. CV's of **1I**·2OTf at different scan rates ([host] = 0.25 mM, *T* = 293 K).

Table S3. Values of E_{pc}, E_{pa}, I_{pc}, I_{pa}, ΔE and I_{pa}/I_{pc} for **1I**·2OTf at different scan rates.

Scan rate/ mV s^{-1}	E_{pa}/ V	E_{pc}/ V	I_{pa}/ µA	I_{pc}/ µA	ΔE_p/ V	I_{pa}/I_{pc}
25	0.291	0.071	1.021	1.016	0.22	1.005
50	0.269	0.079	1.515	1.553	0.19	0.976
75	0.269	0.078	2.046	1.844	0.191	1.109
100	0.271	0.081	2.259	2.521	0.19	0.896
200	0.279	0.083	3.286	3.225	0.196	1.019
400	0.279	0.096	4.842	4.771	0.183	1.015
600	0.276	0.105	6.159	5.913	0.171	1.042
800	0.276	0.115	6.968	7.493	0.161	0.929

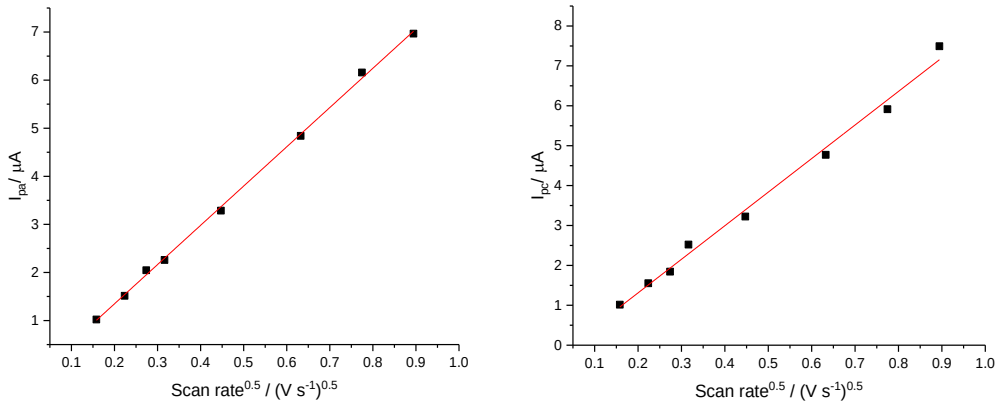

Figure S55. Plots of (left) I_{pa} and (right) I_{pc} against (scan rate)$^{1/2}$ for **1I**·2OTf.

HB Cu(II)-tripod, 1H·2OTf

Studies performed in 0.05 M KPF_6 in pure H_2O.

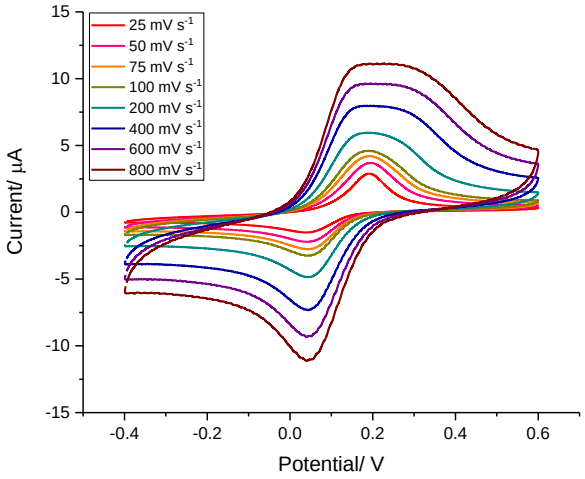

Figure S56. CV's of **1H**·2OTf at different scan rates ([host] = 0.25 mM, *T* = 293 K).

Table S4. Values of E_{pc}, E_{pa}, I_{pc}, I_{pa}, ΔE and I_{pa}/I_{pc} for **1H**·2OTf at different scan rates.

Scan rate/ mV s^{-1}	E_{pa}/ V	E_{pc}/ V	I_{pa}/ µA	I_{pc}/ µA	ΔE_p/ V	I_{pa}/I_{pc}
25	0.191	0.039	2.726	1.667	0.152	1.635
50	0.19	0.037	3.507	2.395	0.153	1.464
75	0.191	0.044	3.918	3.304	0.147	1.186
100	0.191	0.042	4.244	3.640	0.149	1.166
200	0.193	0.044	5.476	5.355	0.149	1.023
400	0.196	0.044	7.406	7.919	0.152	0.935
600	0.205	0.044	9.198	9.781	0.161	0.940
800	0.203	0.041	10.728	11.501	0.162	0.933

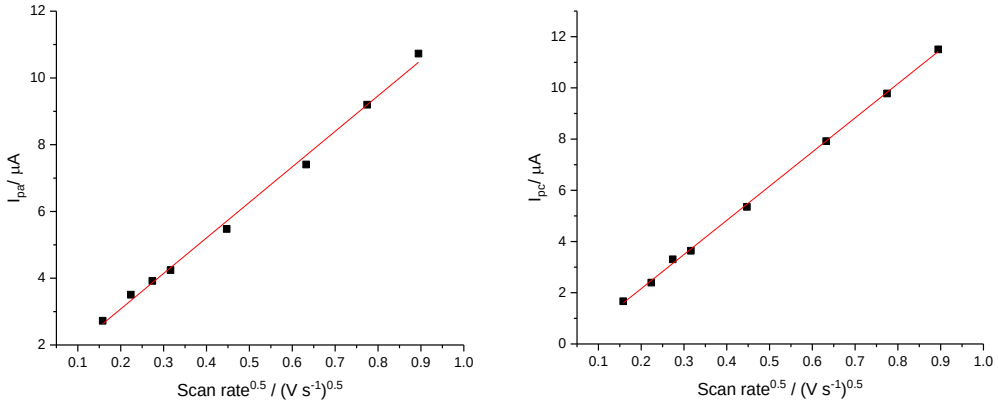

Figure S57. Plots of (left) I_{pa} and (right) I_{pc} against (scan rate)$^{1/2}$ for **1H**·2OTf.

S8. References

1 B.-Y. Lee, S. R. Park, H. B. Jeon and K. S. Kim, *Tetrahedron Lett.*, 2006, **47**, 5105–5109.

2 T. Zhang and E. V. Anslyn, *Tetrahedron*, 2004, **60**, 11117–11124.

3 T. Shiraki, A. Dawn, Y. Tsuchiya and S. Shinkai, *J. Am. Chem. Soc.*, 2010, **132**, 13928–13935.

4 J. Chao, W.-Y. Huang, J. Wang, S.-J. Xiao, Y.-C. Tang and J.-N. Liu, *Biomacromolecules*, 2009, **10**, 877–883.

5 T. Bunchuay, A. Docker, A. J. Martinez-Martinez and P. D. Beer, *Angew. Chem. Int. Ed.*, 2019, **58**, 13823–13827.

6 M. J. Langton, S. W. Robinson, I. Marques, V. Félix and P. D. Beer, *Nat. Chem.*, 2014, **6**, 1039–1043.

7 P. Thordarson, *Chem. Soc. Rev.*, 2011, **40**, 1305–1323.

8 S. L. Tobey and E. V. Anslyn, *J. Am. Chem. Soc.*, 2003, **125**, 14807–14815.

9 R. Oliveira, S. Groni, C. Fave, M. Branca, F. Mavré, D. Lorcy, M. Fourmigué and B. Schöllhorn, *Phys. Chem. Chem. Phys.*, 2016, **18**, 15867–15873.